ANL-76-71

ANL-76-71

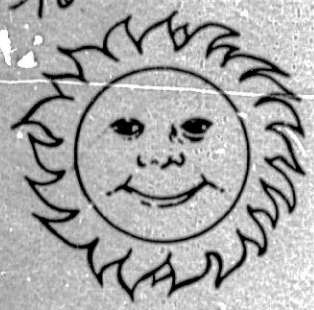

DEVELOPMENT AND DEMONSTRATION OF COMPOUND PARABOLIC CONCENTRATORS FOR SOLAR THERMAL POWER GENERATION AND HEATING AND COOLING APPLICATIONS

Progress Report for the Period
July—December 1975

by

John W. Allen, Norman M. Levitz, Ari Rabl,
Kent A. Reed, William W. Schertz,
George Thodos, and Roland Winston

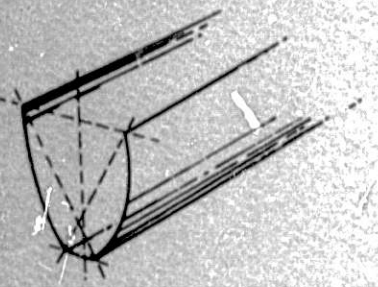

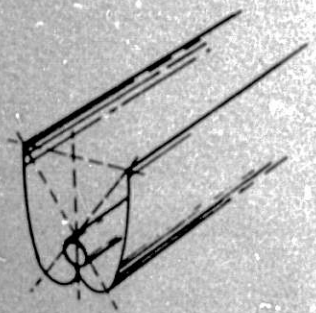

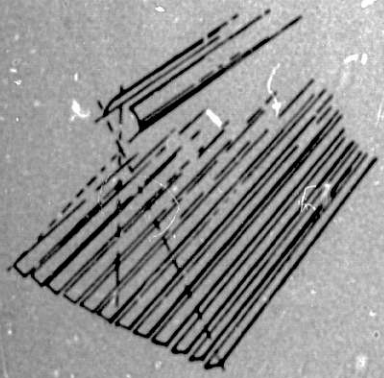

ARGONNE NATIONAL LABORATORY, ARGONNE, ILLINOIS
Prepared for the Division of Solar Energy
U.S. Energy Research and Development Administration
under Contract W-31-109-Eng-38

Printed in the United States of America
Available from
National Technical Information Service
U. S. Department of Commerce
5285 Port Royal Road
Springfield, Virginia 22161
Price: Printed Copy ~~$5.00~~ $5.25; Microfiche $3.00

Distribution Category:
Solar Thermal (UC-62)

ANL-76-71

ARGONNE NATIONAL LABORATORY
9700 South Cass Avenue
Argonne, Illinois 60439

DEVELOPMENT AND DEMONSTRATION OF COMPOUND PARABOLIC CONCENTRATORS FOR SOLAR THERMAL POWER GENERATION AND HEATING AND COOLING APPLICATIONS

Progress Report for the Period
July—December 1975

by

John W. Allen, Norman M. Levitz, Ari Rabl,
Kent A. Reed, William W. Schertz,
George Thodos,* and Roland Winston

Solar Energy Group

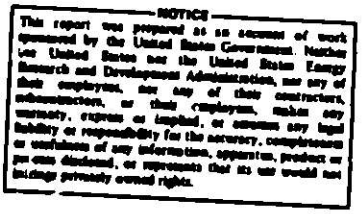

*Visiting Professor, Northwestern University

TABLE OF CONTENTS

TABLE OF CONTENTS (contd)

LIST OF FIGURES

LIST OF FIGURES (contd)

LIST OF TABLES

k	Thermal conductivity
k_1	Heat absorbed per unit length
k_2	Overall heat transfer coefficient between tube side and annulus side of concentric flow heat exchanger
k_m	Thermal conductivity of tube wall
L	Length (cm)
l	Thickness of tube wall
$\dot{m}$	Mass flow rate of heat transfer liquid
n	Index of refraction
P_i	Inside tube perimeter
P_m	Mean tube perimeter
P_o	Outside tube perimeter
$\vec{p}$	Canonical momentum vector
q	Heat
R	Thermal resistance
r_i	Inside radius
r_o	Outside radius
$\vec{r}$	Position vector
S	Total (direct beam + diffuse) insolation falling on the collector plane as measured by a pyranometer
ρ_a	Signal detected by detector of light box
A	Cross-sectional area for unit length
A_1	Input aperture area
A_g	Area of glass
A_r	Area of receiver
C	Concentration ratio
c_p	Specific heat of liquid
D	Tube diameter
D_1	Outside diameter of inner tube of annulus
D_2	Inside diameter of outer tube of annulus
D_e	Effective diameter of annulus = $D_2 - D_1$
d_1	Entrance aperture width
d_2	Exit aperture width
$\vec{\ell}$	Angular momentum vector
F_{rg}	Form factor for receiver-glass radiative coupling
$F(\theta)$	Fraction of radiation incident on inlet aperture that is absorbed by receiver.
$f(\theta)$	Angular acceptance characteristic
h_i	Inside film coefficient
h_o	Outside film coefficient
I_{abs}	Radiation absorbed
$I_{in}(\theta_{in})$	Radiation incident on aperture at angle θ_{in}
$\vec{s}$	Direction vector
T	Fluid temperature, annulus side
T_1	Inlet fluid temperature, annulus side
T_a	Temperature of ambient
T_g	Temperature of glass envelope
T_r	Temperature of receiver
T_{sky}	Temperature of sky
T_∞	Air temperature
ΔT	Temperature above ambient
t	Fluid temperature, tube side
U	Heat loss coefficient based on aperture area
U_{back}	Heat loss coefficient for the back of the collector
U_{day}	Daytime overall heat loss coefficient
U_{night}	Heat loss coefficient based on aperture area for indoor or nighttime testing
α	Absorptivity of receiver
δ	Fraction of insolation accepted by CPC
η	Efficiency
η_o	Optical efficiency
$\langle n \rangle$	Average number of reflections for light going from entrance aperture to receiver
θ_{max}	Acceptance half angle
θ	Angular coordinate (Eq. 33-37)
θ	Angle of incidence of radiation at aperture (Eq. 17-26)
μ	Viscosity of fluid
μ_s	Viscosity of fluid at metal surface
ρ	Radial coordinate (Eq. 33-37)
ρ	Reflectivity
σ	Stephen-Boltzman constant
τ	Transmissivity of single cover and glass jacket
$\tau_R(\theta)$	Effective transmissivity of CPC for radiation incident at angle θ which can reach absorber
$\tau_{R\ out}(\theta)$	Effective reflectivity of CPC for radiation which cannot reach absorber
$\bar{\tau}_R$	Effective average transmissivity of CPC for diffusely incident radiation which can reach the absorber

DEVELOPMENT AND DEMONSTRATION OF COMPOUND PARABOLIC CONCENTRATORS FOR SOLAR THERMAL POWER GENERATION AND HEATING AND COOLING APPLICATIONS

by

John W. Allen, Norman M. Levitz, Ari Rabl, Kent A. Reed, William W. Schertz, George Thodos*, and Roland Winston

ABSTRACT

Work on the development of Compound Parabolic Concentrators (CPC) during the reporting period is described. A tenfold concentrator with a cavity receiver was constructed and tested. The optical efficiency was very good (65%), but the thermal performance was degraded by heat losses of the cavity receiver.

A 20 ft^2 (1.86 m^2) concentrating collector (5.3x) fabricated by Chamberlain Manufacturing Corp. under contract with Argonne National Laboratory has been tested for thermal and optical performance, and the optical efficiency was excellent (68%). In this collector, aluminum extrusions were used to define the CPC shape and provide the fluid-flow path.

A 30 ft (9.14 m) long collector (10x) has been designed and is being built for daily-cycle testing. The expected performance of this collector has been evaluated.

The conceptual design of a lightweight collector using evacuated glass tubes around the absorber is presented. Various construction techniques for use with low-cost materials, such as plastics, are being evaluated for this collector.

Optical design studies of Compound Parabolic Concentrators for tubular absorbers and for use as secondary concentrators are discussed. Comparison of the CPC with tube and the CPC with one-sided flat absorber shows that the tubular configuration is preferable not only because of lower heat losses but also because of lower collector cost. For tracking concentrators with line focus, the use of second-stage concentrators is found to be cost

*Visiting Professor from Northwestern University, Evanston, Illinois 60201.

effective; the CPC is found to be significantly better for this application than a V-trough.

A summary of the results of subcontracts described in the previous progress report are presented, and the influence of these results on ANL programs is noted.

I. INTRODUCTION

The Compound Parabolic Concentrator (CPC) is a nonimaging optical-design concept for maximally concentrating radiant energy onto a receiver. The design incorporates a trough-like reflecting wall channel by which radiant energy is concentrated to the maximum allowed by physical principles. This maximum concentration corresponds to a relative aperture (f/number) of 0.5, which is well beyond the limit for imaging collectors. Consequently, for concentrations up to about 10, diurnal tracking is not needed. The sun remains within the angular field of view of the stationary collector for one entire day (annual average of 8 hr). Radiation is collected over an entrance aperture of width d_1 and angular field of view of $2\theta_{max}$, and concentrated onto an exit aperture of width d_2, where $d_1/d_2 = 1/\sin \theta_{max}$.

All CPC designs are characterized by a large angular field of view and a high, uniform-throughput efficiency (the average number of reflections is < 1.5 for concentrations < 10). In many areas of solar-energy technology where optical concentration is indicated, the CPC design offers significant advantages such as the elimination of tracking requirements, which has important consequences. The flexibility of the concept permits advantageous application to many areas of solar-energy technology including heating and cooling, process heat, thermal power generation, and photovoltaic power production.

The design and construction of solar collectors based on the CPC concept for power generation cycles and process heat applications have progressed to the point that the optical characteristics and design requirements are relatively well known. The design of the absorber for thermal uses of the optically concentrated energy requires careful attention to avoid energy loss and performance degradation.

Considerable effort has been devoted to determining the suitability of materials and fabrication techniques for the mass production of reflectors for CPC solar collectors. The effort is oriented toward the use of low-cost materials, such as plastics, foams, and thin sheet metal, which, when combined with appropriate forming techniques, will lower the cost of producing reflector surfaces. Some of these materials require that the hot absorber tube be thermally isolated from the mirror surface; therefore,

investigations have begun on the use and design of an evacuated tube for insulation around the absorber and on the coupling of such absorbers to reflectors.

II. 10x COLLECTOR DESIGN

A. Description of Collector Construction

The 10x CPC array for daily-cycle testing has a 40 ft^2 (3.72 m^2) frontal area and a design goal of operating temperatures of 350-450°F (176-232°C). It was originally conceived as a 6 ft x 10 ft (1.83 m x 3.05 m) array composed of ten 6 ft (1.83 m) long channels, with each channel having an 8 in. (20.32 cm) aperture (See. Fig. 1). The disadvantage of this array is that each channel requires two end mirrors. With a nontracking collection system, the extra reflections due to end mirrors would decrease collection efficiency. The reflectivity (ρ) of the Kinglux* aluminum mirrors is 0.85. The loss that can be attributed to the end-mirror reflections is most prominent at the beginning and end of the day, which can be minimized by reducing the number of end reflections (i.e., by making the collector longer).

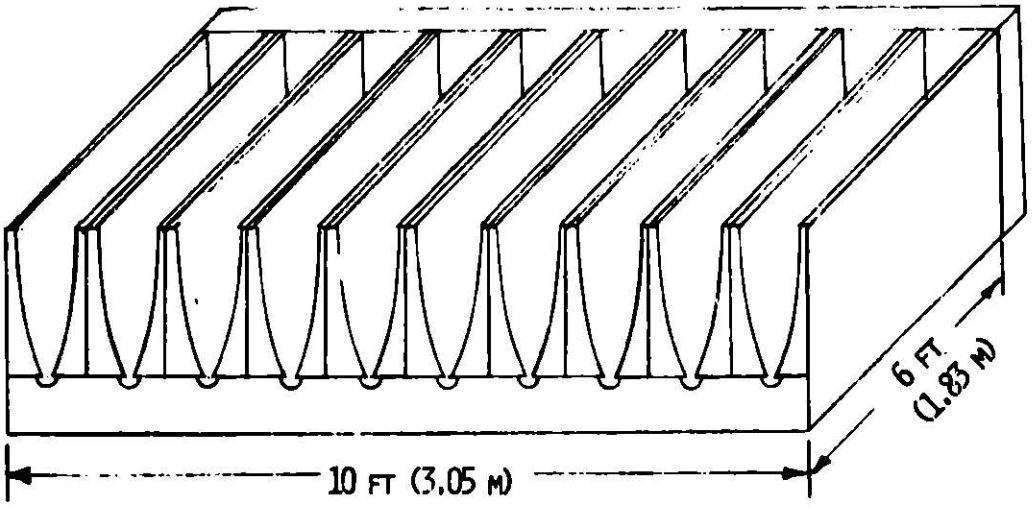

FIG. 1 ORIGINAL 10x CPC ARRAY

To limit the losses due to end mirrors, the design was modified to a 2 ft x 30 ft (0.61 m x 9.14 m) array consisting of two channels, 30 ft (9.14 m) long, with each channel having an 8 in. (20.32 cm) front aperture (see Fig. 2). This configuration reduced the total number of end mirrors from 20 to 4.

*Product of Kingston Industries, 207 E. 37th St., New York, New York 10016.

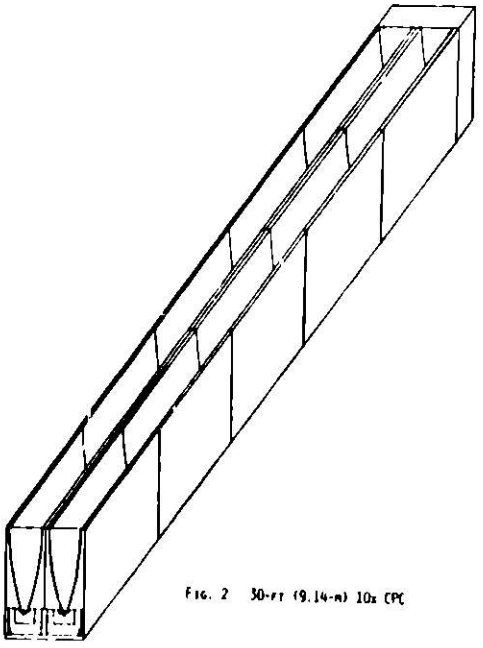

FIG. 2 30-FT (9.14-M) 10x CPC

To facilitate construction and handling, the 30 ft (9.14 m) array was designed to be made of 5 modules, each module being 6 ft (1.83 m) long (see Fig. 3). Insulation sections 1 ft (30.4 cm) long are attached at the ends of the collector.

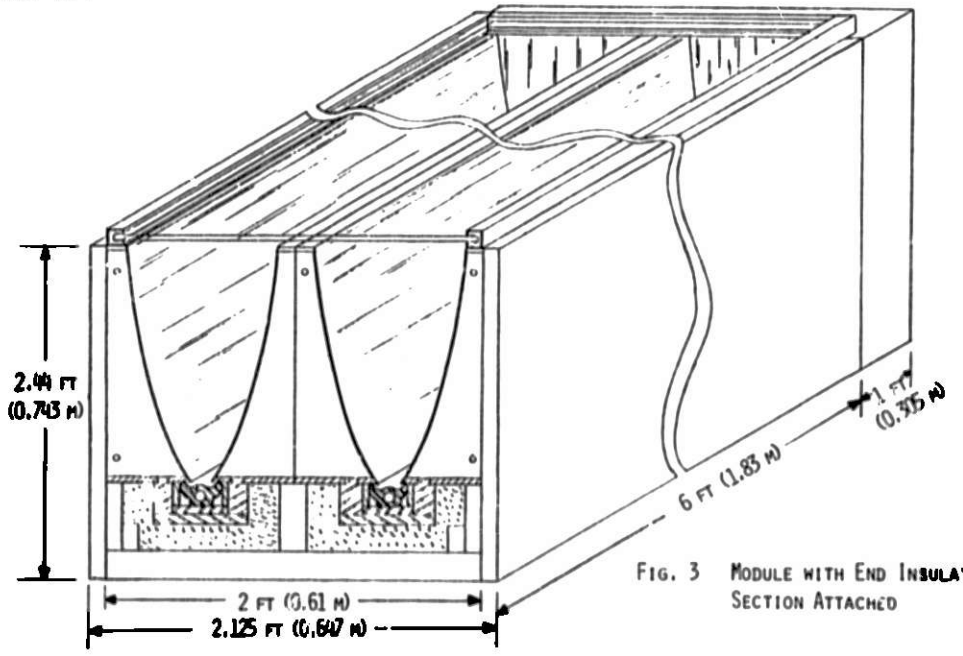

FIG. 3 MODULE WITH END INSULATION SECTION ATTACHED

The modules are constructed by using 3 ft (0.91 m) long rib subsections made up of 5 plywood ribs with pieces of G-10* plastic on the top and bottom to hold the mirrors in the CPC shape (See Fig. 4); the bottom G-10 plate

*Fiberglass-reinforced epoxy, product of Synthane Corp., Oaks, Pennsylvania.

actually is two strips separated by an air gap to reduce the thermal conduction path from the receiver to the exterior as shown in Fig. 4. Two subsections are bolted together to form a 6 ft (1.83 m) long rib section. Four rib sections are then used to form a 6 ft (1.83 m) long module containing two channels (see Fig. 3). The two center rib sections are bonded together back to back. The center ribs are supported by a 2 x 6 board bonded to the 1 in. (2.54 cm) thick plywood bottom. The two outside rib sections are attached to the 3/4 in. (1.9 cm) thick plywood sides. The bottom aperture spacing is maintained with U-shaped phenolic brackets. These U-brackets also support the receivers in proper alignment to the mirrors. The top aperture spacing is maintained by 1/8 x 1/4 in. (0.32 x 0.64 cm) steel spacer bars.

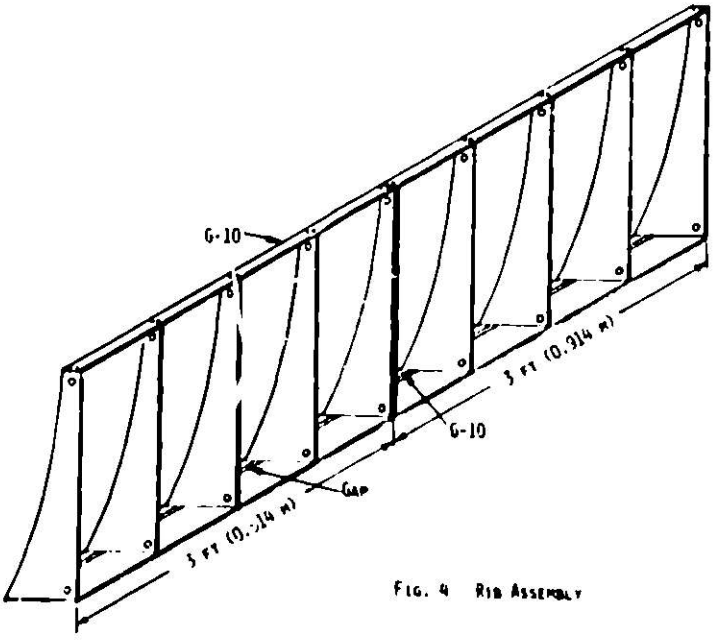

FIG. 4 RIB ASSEMBLY

The cover glass is composed of 6 ft x 2 ft x 3/8 in. (1.82 m x 0.914 m x 0.95 cm)-thick glass plates supported by an aluminum frame. The glass is held in place in the aluminum frame with rubber gasketing. The joints between the glass plates are sealed, using hollow plastic tubing held in place with clear silicone rubber. This method should result in minimum blockage of the frontal area. The tubing-silicone rubber seal was selected to allow for the thermal expansion of the glass as the cover heats up in the sun. The cover glass is expected to be 50°F (28°C) hotter than the aluminum frame when the receiver is at 450°F (232°C).

B. Reflector Assembly

The module design utilizes pins in one end and holes in the other to allow alignment of one module to the next. Brackets on the side of the modules are used to rigidly fasten the modules together.

Tests have been run to determine the best method for attaching the mirrors to ribs with the least distortion due to thermal expansion. The Kinglux aluminum mirror sheets are 18 in. x 23 in. (45.7 x 58.4 cm). They may be expected to heat up to ∿170°F (∿77°C) when illuminated in sunlight; this will result in a linear expansion of about 1/16 in. (0.16 cm) over a 20-in. (50.8-cm) length. The test section mirrors were attached using (1) silicone rubber, (2) regular epoxy with epoxy-fiberglass reinforcement between rib sections, (3) slotted aluminum tabs held on by pop rivets and (4) slotted aluminum tabs held on by rubberized epoxy. The regular epoxy with epoxy-fiberglass reinforcement broke loose from the Kinglux sheets when heated to 175°F (80°C). The silicone rubber held the aluminum sheets to the wooden ribs, but since the metal sheets could not move, they were severely distorted after thermal cycling. The slotted aluminum tabs held with pop rivets were the most effective. They allowed the Kinglux sheets to move relative to the wooden ribs without causing distortion, even after temperature cycling up to a maximum temperature of 225°F (107°C). The metal tabs that were held onto the aluminum sheet by rubberized epoxy failed because of stretching of the epoxy during thermal cycling.

Slotted aluminum tabs held with pop rivets were selected as the best method of attachment. The slots are cut parallel to the ribs to allow vertical expansion, and the tabs are spaced away from the rib by fiber washers to allow for horizontal expansion by bending of the metal tabs. Six tabs are used along each rib. The reflective sheets are spaced approximately 1/16 in. (0.16 cm) apart at room temperature to allow for horizontal expansion.

The mirror curvature at the bottom of the reflector assemblies initially did not conform to the CPC shape in the region between the ribs. To correct this problem, the bottom 2.5 in. (6.35 cm) of the reflective aluminum sheets were rolled to the approximately correct radius. This prebending of the sheet aids in maintaining the correct shape between the ribs.

C. Receiver Design

The receiver chosen for the 10x CPC was manufactured by Chamberlain Manufacturing Corporation. These receivers are the same as those used in the 5.3x collector constructed for ANL by Chamberlain and described in Section IV. A cross section of the extruded aluminum receiver is shown in

Fig. 5. The shape of the absorbing surface results in a "cavity" effect and increases the absorptivity slightly. The receivers are cut 6.021 ft (1.835 m) long. This will allow the receivers, when assembled, to extend beyond the end mirrors when the receivers are at ambient temperature. The receivers in the center module are firmly attached near their center section with screws. The receivers in the other modules are allowed to slide in the phenolic U-brackets. The 30 ft (9.14 m) length of 6063-T5 aluminum is expected to expand ∿2 in. (∿5 cm) when heated from 50-500°F (10-260°C) (maximum temperature anticipated). With the 30 ft (9.14 m) receiver held at its center, each end will move 1 in. (2.54 cm).

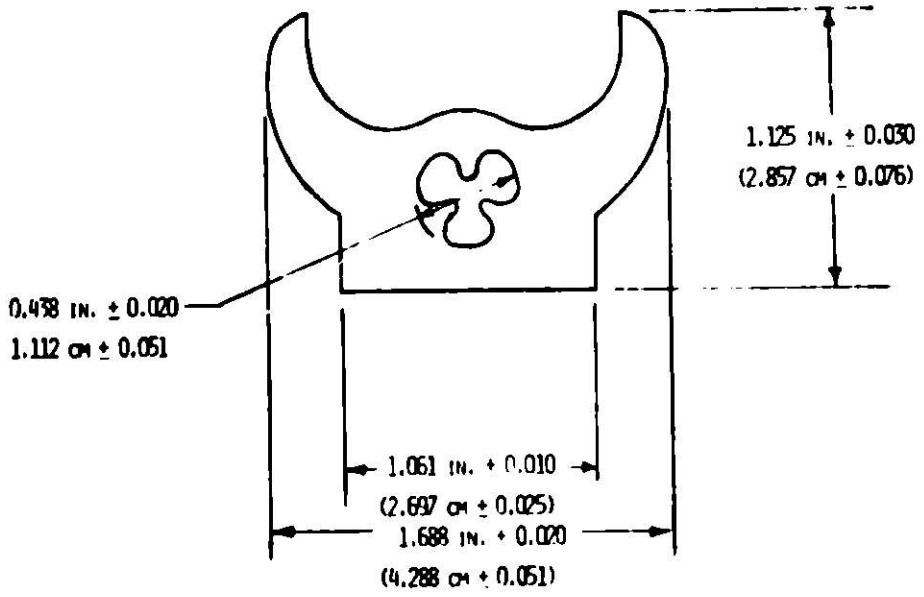

FIG. 5 EXTRUDED ALUMINUM RECEIVER

The interconnection of the 6 ft (1.83 m) receivers is accomplished by aluminum tubing and tubing connections, using aluminum Swagelok to 1/8 in. (0.32 cm) NPT fittings located 1 in. (1.83 m) from the end of each receiver. The ends of the flow channels in each 6 ft (1.83 m) receiver are drilled and tapped for 1/4 in. (0.64 cm) NPT. The ends of each intermediate receiver section will be plugged with aluminum socket head plugs to allow butt-joining the receiver sections. The connections to the ends of the 30 ft (9.14 m) long interconnected receivers will be made using the 1/4 in. (0.64 cm) NPT tapped holes in the ends of the flow channel.

The receivers in the two channels will have different absorbing surfaces to allow a direct comparison of the performance of the surfaces. The receiver in one of the channels will have a black-chrome selective-surface

finish. The surface has been applied by Olympic Plating of Cleveland, Ohio, and was done under contract to Chamberlain Manufacturing Corporation. This black-chrome finish should have an absorption (α) of 0.90 and an emissivity (ϵ) of 0.10. However, the emissivity (ϵ) is expected to increase to 0.2 at 450°F (232°C).[1] The receiver in the other channel will have a nonselective flat black finish applied by Chamberlain Manufacturing Corporation with an α and $\epsilon \approx 0.9$-0.95. The sides and bottom of the nonselective receiver were polished, and the top was coated with Caldwell flat black No. 129-38^f paint which was then cured at 350 ± 10°F (176 ± 5.6°C) for 15 to 30 minutes. This paint is manufactured by Caldwell Chemical Coatings Corporation, 209 Ardmore Road, Fayetteville, Tennessee. The maximum temperature capability for the paint is 900°F (482°C) without blistering.

D. Mirror Insulation

The insulation of the CPC modules was studied to limit the heat losses from the receiver. Polyurethane was considered for the insulation behind the mirrors, but was rejected for two reasons: (1) the maximum operating temperature could exceed the temperature limitation of polyurethane (250°F or 121°C); and (2) during the curing process, polyurethane foam develops forces that are capable of bending the mirrors out of their proper curvature. The insulation chosen was rockwool, which has a thermal conductivity of 0.022 Btu ft/ft^2 hr°F (3.8×10^{-4} W/cm°C) compared to 0.012 Btu ft/ft^2 hr°F (2.07×10^{-4} W/cm°C) for polyurethane, and has a maximum temperature capability of 1300°F (704°C).

E. Receiver Insulation

The G-10 pieces at the bottom of the ribs are made in two pieces, with a gap between them to increase the thermal resistance, as shown in Fig. 6. The resistance, R, was calculated by $R = L/Ak$, where L is the thickness, A is area, and k is the thermal conductivity, as shown in Table 1. The heat loss by conduction through the G-10 pieces for a 400°F (204°C) receiver temperature and a 50°F (10°C) ambient is calculated to be 2.2 Btu/hr lin. ft (0.2 W/lin. cm). This corresponds to a loss of 3.3 Btu/hr per ft^2 of frontal area (0.001 W/cm^2).

The heat lost through the insulation behind and to the sides of the receiver is an important loss which can be minimized by careful material

selection. To evaluate different insulations, the assumption was made that the receiver insulation could be considered as a composite cylindrical insulation for which $R = \ln(r_o/r_i)/2\pi\ k\ l$, where r_o is the outside radius, r_i is the inside radius, k is the conductivity, and l is the receiver length. The heat lost by conduction through the insulation is then equal to $q = T_i - T_o/\Sigma R$.

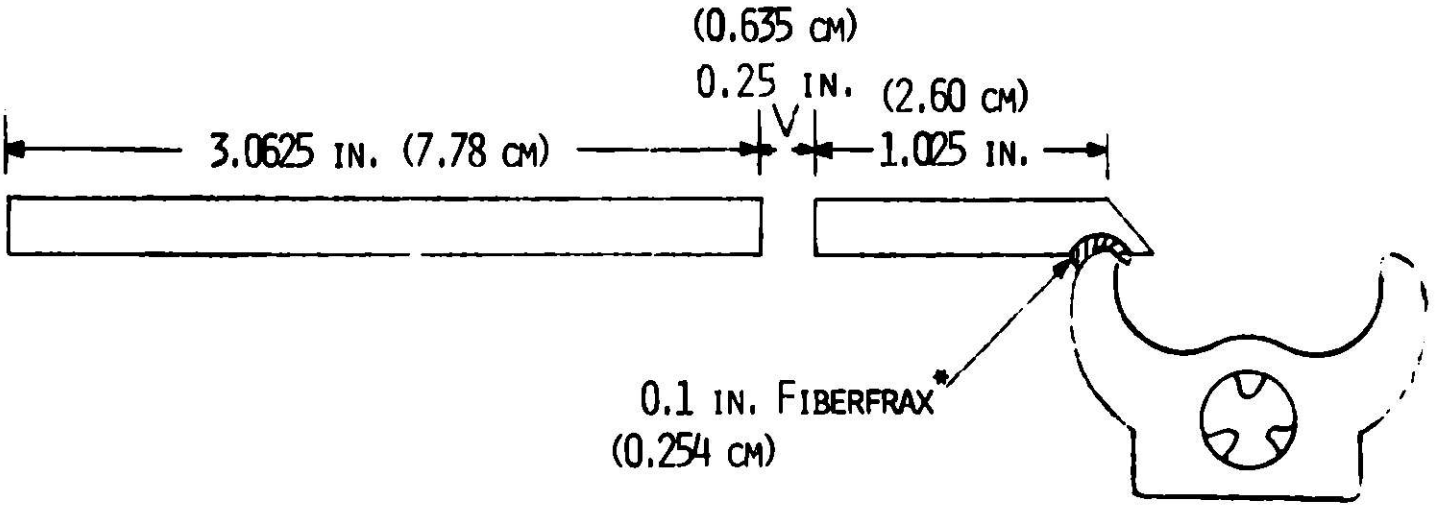

FIG. 6. INSULATION OF RECEIVER SUPPORT

TABLE 1. Thermal Resistance

	L	A	k	R
	in(cm)	$\frac{ft}{lin\ ft}\left(\frac{cm^2}{lin\ cm}\right)$	$\frac{Btu\ in.}{hr\ ft^2°F}\left(\frac{W}{cm°C}\right)$	$\frac{hr°F}{Btu/lin\ ft}\left(\frac{°C}{W/lin\ cm}\right)$
Fiberfrax	0.1(0.254)	0.0208(0.634)	0.3(0.00043)	16(926)
1st G-10	1.25(3.175)	0.0208(0.634)	2.0(0.0028)	30(1737)
Rockwool in gap	0.25(0.61)	0.0208(0.634)	0.47(0.00067)	25.5(1476)
2nd G-10	3.625(9.21)	0.0208(0.634)	2.0(0.0028)	87(5037)

Total $R = 158.5\ \frac{hr°F}{Btu/lin\ ft}\left(9148\ \frac{°C}{W/lin\ cm}\right)$

*A product of Carborundum Co., Niagara Falls, New York

The insulation originally considered was 2 in. (5.08 cm) of Foamglas* [which has a k value of 0.05 Btu ft/hr ft^2°F (8.65×10^{-4} W/cm°C) at 350°F (1.77°C)] combined with 2 in. (5.08 cm) of polyurethane. The maximum acceptable temperature at the Foamglas-polyurethane interface is the temperature limit of polyurethane (250°F, 121°C). One of the limitations of this composite insulation is that the maximum allowable receiver temperature is only 320°F (160°C) for a 250°F (121°C) interface. Increasing the Foamglas to 3 in. (7.62 cm) while decreasing the polyurethane to 1 in. (2.54 cm) lowers the interface temperature so that the receiver can operate at 500°F (260°C), but this increases the heat loss (based on frontal area) from 28.5 Btu/hr ft^2 (0.0089 W/cm^2) to 45 Btu/hr ft^2 (0.0142 W/cm^2).

An improved insulation was chosen for high-temperature operations, i.e., 2 in. (5.08 cm) of Microtherm backed with 2-in. (5.08 cm) of polyurethane foam. Microtherm is manufactured by Micropore International Ltd. of England, and has a thermal conductivity of 0.012 Btu ft/hr ft^2°F (2.07×10^{-4} W/cm°C). The maximum operating temperature for Microtherm is 1832°F (1000°C). The Microtherm-polyurethane insulation should have a heat loss of only 15 Btu/hr per ft^2 of frontal area (0.00473 W/cm^2) at 500°F (260°C) operating temperature. This is considered to be an acceptable back loss for this collector.

F. Predicted Performance of 10x Collector

The computer model SOLAR-CPC has been used to predict the performance of the 10x CPC collector. This model is based on the methods described in the report "Optical and Thermal Properties of Compound Parabolic Concentrators" to be published in *Solar Energy*. In addition to the radiation and convection modes of heat loss through the front of the collector, conduction losses through the back and sides are incorporated by means of a lumped parameter, U_{back}. The back-loss calculations were discussed in the preceding section on receiver insulations. The values obtained were used in the computer program for U_{back}. The model also accounts for the decrease in heat losses due to the warming of the mirrors because of absorption of solar radiation. Since both nonselective and black chrome absorber coatings will be employed in the 10x CPC, the program has been run for both cases. The predicted performance curves for the 30 ft (9.15 m) collector are shown in Fig. 7 for both the selective and nonselective receivers. For example at ΔT = 300°F

*A product of Pittsburgh Corning Co., Pittsburgh, Pennsylvania.

(166°C), the efficiency should be 38% for the black chrome, 32% for the nonselective black surfaces at an insolation of 300 Btu/ft^2 hr (0.0945 W/cm^2).

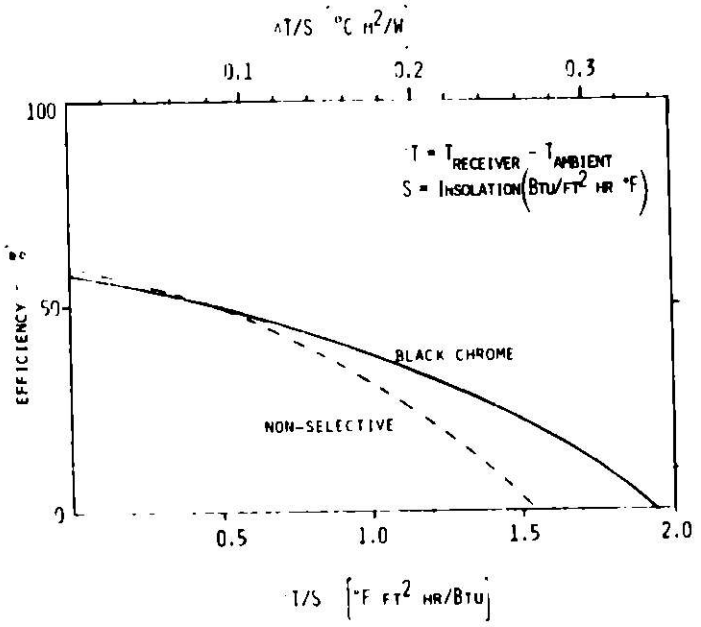

FIG. 7 EXPECTED PERFORMANCE OF 10X CPC

III. LIGHTWEIGHT COLLECTOR DESIGN

A. Description of Collector Concept

The cost of CPC collectors is very dependent upon the cost of the mirror surfaces. This was stressed by the goal studies by A. D. Little and Bechtel[2,3] and by the study for photovoltaic applications by Mobil-Tyco.[4] The goal studies indicated that the unique features of the CPC should allow attainment of operating temperatures of from 350-450°F (176-232°C) without the need for diurnal tracking, but that periodic adjustment would be required. The use of an evacuated receiver and a selective absorber coating is considered necessary to obtain the high-temperature performance.

A program to design a CPC-type collector that utilizes a selective surface absorber in an evacuated glass tube, as well as low-cost lightweight reflectors, was initiated as a result of ANL's earlier experimental program and the recommendations of the goal studies. The use of an evacuated glass housing around the absorber thermally decouples the mirror surfaces from the absorber and allows the use of a broad range of low-cost materials as potential mirror materials. These include plastics, glass, thin sheet-metal with plastic reflector film overcoatings, as well as conventional aluminum sheets. The procedure for accomplishing the design of a collector using lightweight, low-cost materials with an evacuated glass housing was to evaluate the requirements of each component and the interaction between the components to arrive at a design that has good potential for mass manufacture at low cost. The initial version of the collector resulting from this approach is shown in Fig. 8. This collector utilizes lightweight thermoformed plastic mirror sections that have been vacuum-metallized. These mirrors concentrate the energy onto the absorber fin inside an evacuated glass tube. A thermoformed plastic container with molded-in reinforcement ribs that also support the absorber tube contains the reflector-absorber assemblies and provides the weatherproof enclosure required. The design and analysis of each component of the collector have been started during this reporting period.

B. Lightweight Reflectors

The use of glass plates sagged over a steel mold to obtain the CPC shape as reported in the previous semiannual report[5] was not successful because of poor shape definition.

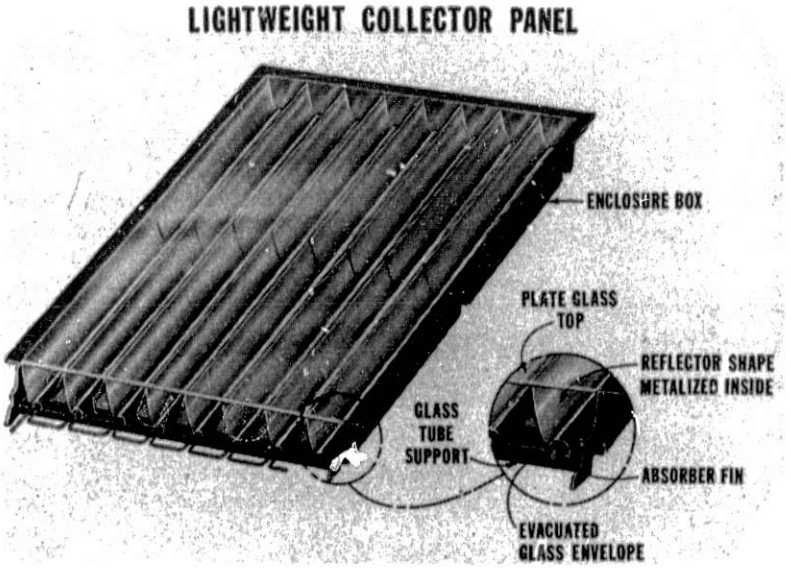

FIG. 8 LIGHTWEIGHT COLLECTOR PANEL

The glass surface did not follow the mold surface precisely; therefore, the acceptance angle for the collector was reduced. This fabrication approach has been deferred at the present time because of the large tooling requirements that would be required to make acceptable glass reflectors. The use of thermoformed plastic reflectors is being investigated as an alternative method of making lightweight mirrors.

To evaluate the ability of thermoformed plastics to conform to the mold surface, an epoxy reflector bar from an old 3x collector (reported in ANL-75-42) was used as a male mold. This allowed a quick test of the thermoforming process without the fabrication expense of a mold. The epoxy bar was 24 in. (61 cm) long by 3 in. (7.62 cm) high and was 1.5 in. (3.81 cm) wide at the base. The bar was mounted on a wooden base. A 0.005 in. (0.0127 cm) slot was located at the base-bar junction by using periodic brass shims. This slot was connected to the vacuum source to remove air from the space between the mold and the hot plastic sheet. A sheet of polyvinylchloride (PVC) plastic that was 0.020 in. (0.51 cm) thick was then clamped in a frame, heated in an oven, and placed over the mold with the vacuum source on. The experiment was repeated using acrylonitrilebutadiene-styrene (ABS) plastic stock. The thermoformed reflector substrate is shown in Fig. 9. These experiments were performed with the extensive assistance of Jim Spitzer of Plastofilm, Inc., Wheaton, Illinois. The therforming experiments are discussed more fully below.

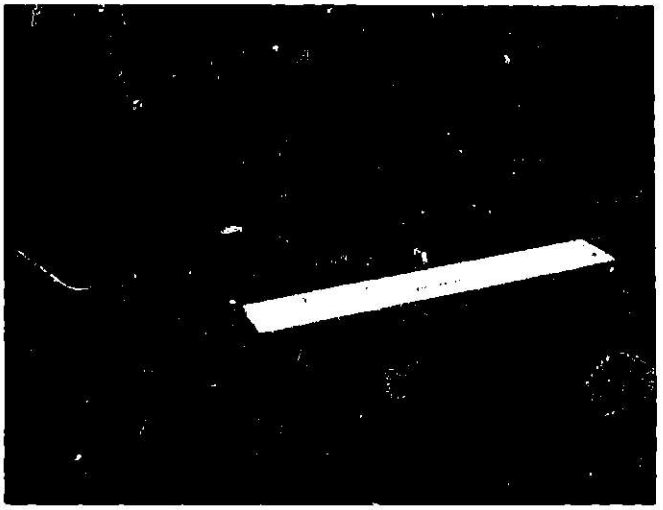

FIG. 9 THERMOFORMED REFLECTOR SUBSTRATE

The resulting hollow, lightweight plastic pieces were vacuum-metallized with aluminum and tested on the light box apparatus as described in ANL-75-52. The results of the lightbox tests are shown in Fig. 10 for the PVC plastic. The shape definition of the thermoformed plastic was excellent, with the measured acceptance angle from the formed piece being as good as the mold surface, and being equal to the design value ($\pm \theta_{max}$). The PVC material had a good gloss after metallization, and, therefore, made a good mirror when vacuum-metallized. The ABS plastic was a glossy material

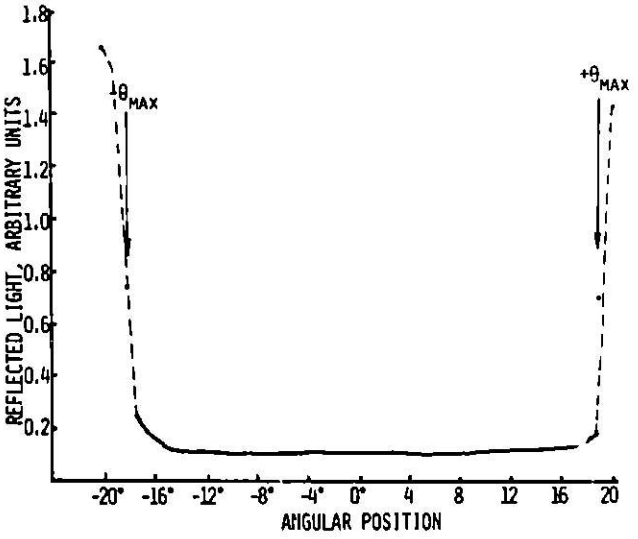

FIG. 10 THERMOFORMED PLASTIC CPC ANGULAR ACCEPTANCE TEST

before thermoforming, but a microroughness that resulted from the stretching of the plastic over the mold reduced the spectral reflectivity to a low value. To use ABS plastic as the substrate, an undercoating material will have to be used to smooth the microroughness of the as-formed piece.

The thermoforming process imposes several limitations on the depth of the part, the width of the entrance aperture, and the thickness of the plastic sheet stock. In cooperation with Plastofilm, Inc., the overall dimensions of the mold for forming a reflector module that would be suitable for use with an evacuated tube receiver were determined. The mold was designed to produce four channels at a time and is shown in Fig. 11. The channel length is 24 in. (0.61 m), the entrance aperture is 4.5 in. (11.43 cm), and the concentration ratio is 3. The semicircular region at the base of the troughs is sized to fit the O.D. of an evacuated-glass-tube receiver described in the next section. The fabrication of the mold from aluminum has been completed and trial parts are scheduled to be fabricated at Plastofilm Industries during the next reporting period.

FIG. 11A MOLD FOR FOUR CHANNEL REFLECTOR

FIG. 11B PLUG ASSIST FOR FOUR CHANNEL REFLECTOR

C. Evacuated Receiver Design

An absorber operating within an evacuated glass envelope (tube) is under development for use with the 3x compound parabolic reflectors mentioned in the previous section. The use of a vacuum significantly reduces convection and conduction losses from the receiver and will allow the reflector surfaces to operate near ambient temperatures. The absorbers presently under

consideration are of metal, are tubular, and may also have a fin. The use of a heat pipe is also being considered. A number of evacuated receiver designs have been suggested, as shown schematically in cross section, in Fig. 12. The options include vertical or horizontal absorbers, once-through fluid flow and flow paths with a return, such as the hairpin or concentric tube arrangement. All receiver designs are compatible with the reflector shapes described in the previous sections. Several evacuated receiver designs are being evaluated analytically; the results of this work are given later in this report.

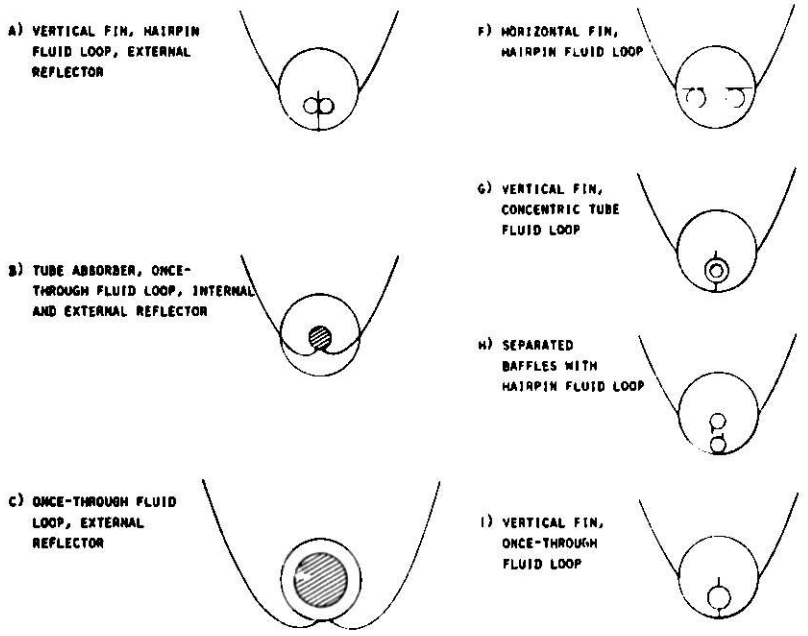

FIG. 12 VARIOUS RECEIVER-REFLECTOR DESIGNS FOR HIGH TEMPERATURE OPERATION WITHIN A VACUUM JACKET

A number of design features and operating parameters for the evacuated receiver assembly have been selected on the basis of a preliminary analysis:

a. Temperature range, 350-450°F (117-232°C).

b. Receiver material: copper, steel, or aluminum.

c. Selective coatings for the front receiver surface.

d. Vertical or horizontal receiver configurations; the design effort is to minimize the area and mass.

e. Commercially available soft-glass tubes are being considered as the prime candidate for the envelope (because of lower cost); however, borosilicate glass will be used for laboratory prototypes.

f. Vacuum below 10^{-4} torr, which eliminates convection and reduces conduction losses markedly; the main heat loss is then by radiation and by conduction through support brackets.

g. The use of Dowtherm A* as a heat-transfer fluid.

h. The use of "getters" to remove residual gases from the tube that may arise from outgassing during operation.

The temperature range of interest is for power-producing applications. Eventually the CPC collector will be coupled to a power cycle, such as a Rankine engine.

The use of selective coatings on receivers to suppress energy loss by infrared radiation has been reported in the literature.[6] Black chrome has been selected for the initial work in this program. Tests are planned to show differences in performance between selective coatings and high-temperature flat-black paints.

Receiver designs include concentric tubes and hairpin loops that have the fluid inlet and outlet at the same end of the glass envelope or a single tube that provides once-through (unidirectional) flow. The latter requires glass-metal seals at both ends of the glass envelope, and the design must allow for the stress resulting from thermal expansion of different materials. The "floating-type" receivers (inlet and outlet at the same end) tend to simplify this situation. The concentric tube design has been selected as a reference design and is undergoing thermal analysis and mockup. The thermal analysis is reported later in this section.

Penetration of the soft-glass tube with a metal receiver-fluid loop requires glass-metal seals; these are not as readily available as KOVAR-borosilicate glass seals. The use of soft glass will require extensive development work. During this reporting period, alloys of nickel and iron (Niron-52), which have expansion coefficients compatible with that of the soft glass, have been obtained. A vendor willing to prepare some glass-metal seals for testing at ANL has been located, and an R-F heating technique will be used. The test specimens will be vacuum-tested at ANL. Assembly of test receivers made of Pyrex (borosilicate) glass and KOVAR seals is also planned. "Getters" are considered necessary to help maintain the vacuum. The practice of depositing these materials is commercial, so no difficulty is expected in having the depositing done, when needed for assembly of the receivers.

---

*Dowtherm A is a product of Dow Chemical Company, Midland, Michigan.

Numerous other factors have been evaluated in developing the receiver design. For example, the vertical fin receiver which has an overall height about equal to the radius of the glass tube will require less material than the horizontal fin receiver which has a width slightly less than the diameter of the tube. However, this must be balanced against the receiver area which should be minimized to reduce radiant energy losses. Preliminary calculations show that the horizontal fin receiver with the fluid tubes on the underside of the baffle (the absorbing surface) has only 2/3 the area of the vertical hairpin configuration and about 83% of the area of the concentric tube unit.

D. Thermal Analysis

Reference 18 describes a method for calculating the heat-transfer performance of an evacuated glass-jacketed absorber. This analysis applies to absorbers which are fixed at one end of the glass jacket while the other end remains unattached to allow for expansion and contraction. This structural design requires that the heat-transfer-fluid flow be countercurrent as shown in Fig. 13.

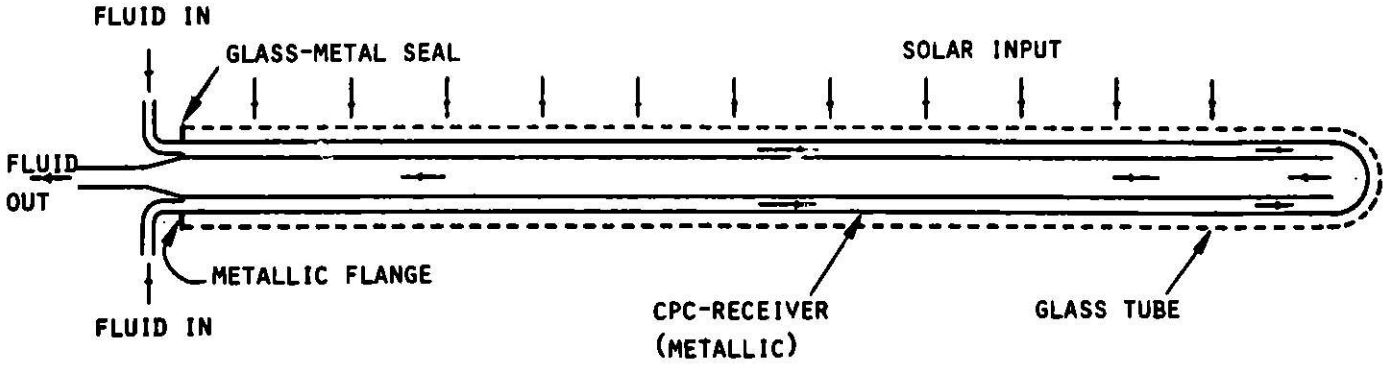

FIG. 13 SCHEMATIC FLOW DIAGRAM FOR THERMAL ANALYSIS

The optical efficiency of this collector using an Alzak* reflecting surface, a cover glass, and a receiver surface treated specifically for high absorptivity and low emissivity has been calculated to be 0.536. The

*Alzak is a product of Alcoa Aluminum Co.

countercurrent performance of the heat-transfer fluid within the receiver has been analyzed mathematically, and effective thermal efficiency values have been calculated and related to the difference in temperature between the receiver temperature within the evacuated glass envelope and the ambient air surrounding this glass jacket.

The use of an evacuated glass jacket minimizes heat losses due to conduction, convection and radiation from the CPC collector. If absolute pressures of 10^{-4} to 10^{-9} mm are established, substantial reduction of convective and conductive losses from the absorber should be realized. The proper application of a selective coating on the exterior surface of the absorber should substantially reduce heat losses from the receiver due to radiation. Therefore, the combined effect of a selectively treated surface and the presence of an evacuated space surrounding the receiver should be effective towards minimizing heat losses from the receiver, and thus effectively increase the thermal efficiency of the collector.

A thermal energy analysis of the countercurrent flow arrangement of the receiver presented in Fig. 13 shows that the temperature of the fluid flowing through the annular section of this heat-exchange facility increases steadily to a maximum value at the end of the receiver; and when the fluid flow is reversed, the temperature decreases steadily until the fluid exits from the receiver. A typical temperature profile for the flow of fluid through the annular-side and tube-side of the receiver is presented in Fig. 14. This temperature reversal results from the thermal short-circuiting experienced in the flow of heat from the fluid inside the tube, through the tube wall and into the fluid flowing countercurrently in the annular space. A thermal energy balance made at a differential length of receiver results in differential equation expressions, which when integrated, produce the following temperature profiles:

$$T = T_1 + \frac{k_1}{\dot{m}c_p} \frac{k_2}{\dot{m}c_p} (2L - x) \frac{x}{2} \quad \text{(annulus-side)}; \tag{1}$$

$$t = t_1 + \frac{k_1}{\dot{m}c_p} \left[1 + \frac{k_2}{2\dot{m}c_p} (2L - x)\right] x \quad \text{(tube-side)} . \tag{2}$$

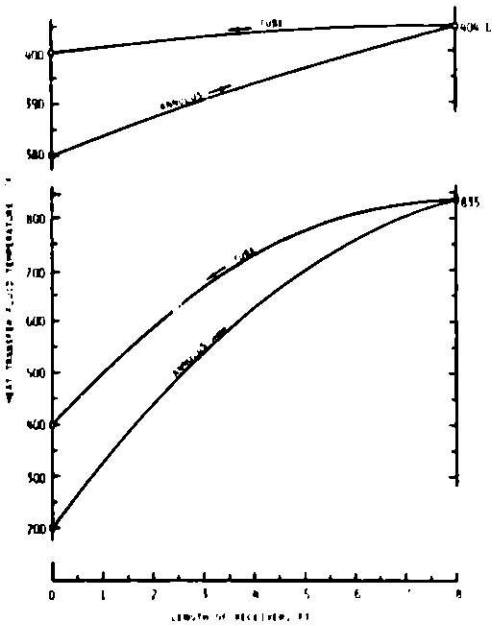

Equations (1) and (2) at x = L, the end of the receiver, become

$$T_L = T_1 + \frac{k_1 L}{\dot{m} c_p} \quad \frac{k_2}{\dot{m} c_p} \quad \frac{L}{2} \quad , \tag{3}$$

and

$$t_L = t_1 + \frac{k_1 L}{\dot{m} c_p} + \frac{k_1 L}{\dot{m} c_p} \quad \frac{k_2}{\dot{m} c_p} \quad \frac{L}{2} \tag{4}$$

where $T_L = t_L$. In Eqs. (1) and (2), the constant k_1 is defined as the incremental radiant energy influx per unit length of receiver ($k_1 = \frac{dQ_1}{dx}$) and k_2 is associated with the overall heat-transfer coefficient between the tube-side and annular-side as follows:

$$k_2 = \frac{dQ_2}{(T - t)dx} \tag{5a}$$

and

$$\frac{1}{k_2} = \frac{1}{h_i p_i} + \frac{\ell}{k_m p_m} + \frac{1}{h_o p_o} \quad , \tag{5b}$$

where h_i and h_o have the usual connotation of inside and outside film coefficients; ℓ and k_m are the thickness and thermal conductivity of the tube wall; and p_i, p_m, and p_o are the inside, mean, and outside tube perimeters.

The expression for the optical efficiency η_o reported by Rabl (Ref. 7) has been applied

$$\eta_o = \gamma \rho^{<n>} \tau \alpha \qquad (6)$$

where

γ = fraction of insolation S accepted by CPC,
ρ = reflectivity of reflecting surfaces,
τ = combined transmissivity of single cover and glass jacket,
α = effective absorptivity of receiver surface, and
$<n>$ = average number of reflections from aperture to receiver surface.

The optical efficiency, for a typical CPC collector accommodated with an evacuated glass-jacketed receiver, becomes

$$\eta_o = 0.92(0.88)^{1.3}(0.85 \times 0.90)(0.90) = 0.536.$$

This value implies that 46.4% of the insolation incident to the aperture of the collector is dissipated before getting to the receiver surface. The fraction of insolation incident on the aperture of the CPC collector that is eventually directed to and absorbed by the receiver is $\eta_o S$, but only a portion of it is retained as useful heat, Q_{useful}, for raising the temperature of the fluid flowing through this unit. The difference, $\eta_o S - Q_{useful}$ is dissipated in the form of a heat loss which is directed from the absorber surface to the glass jacket by the mechanism of radiation. In turn, the glass jacket, whose temperature is correspondingly increased, loses heat to the environment by radiation and by convection to the surroundings. Any conductive heat losses, which can be minimized, can be ignored for this analysis.

The inside and outside film coefficients, required to establish parameter k_2 of Eq. (5b), can be calculated from well-established relationships presented in the literature.[8] For flow inside the tube, the expression

$$\frac{h_i D}{k} = 1.86 \left(\frac{DG}{\mu}\right)^{1/3} \left(\frac{c_p \mu}{k}\right)^{1/3} \left(\frac{D}{L}\right)^{1/3} \left(\frac{\mu}{\mu_s}\right)^{0.14} \tag{7}$$

is used for laminar flow conditions. For flow through the annular cross-sectional area, the outside film coefficient can be determined for laminar flow conditions with the relationship

$$\frac{h_o D_e}{k} = 1.02 \left(\frac{D_e G}{\mu}\right)^{0.45} \left(\frac{c_p \mu}{k}\right)^{0.5} \left(\frac{\mu}{\mu_s}\right)^{0.14} \left(\frac{D_e}{L}\right)^{0.4} \left(\frac{D_2}{D_1}\right) \left(\frac{D_e^3 \rho g \beta \Delta t}{\mu^2}\right)^{0.05} \tag{8}$$

where D_1 and D_2 are the diameters associated with the annular space and $D_e = D_2 - D_1$. The establishment of k_2 requires a trial-and-error procedure wherein a collector efficiency η is assumed to affix $Q_{useful} = \eta S$, $k_1 = Q_{useful}/L$, and for a designated temperature rise of the fluid, $T_1 - t_1$, the product $\dot{m} c_p = Q_{useful}/(T_1 - t_1)$. In addition to this assumed efficiency, η, a value of k_2 is assumed so that the terminal temperature can be established using either Eq. (3) or (4). Either of these expressions should yield the same numerical terminal temperature wherein $T_L = t_L$, regardless of the k_2 value assumed.

The value of the parameter k_2 corresponding to the assumed CPC efficiency is then checked by calculating h_i and h_o using Eqs. (7) and (8) and checking their consistency with k_2 through the use of Eq. (5). If a disparity exists between assumed and calculated values of k_2, the process is repeated using the latest k_2 value in Eq. (3) or (4) to reestablish T_L or t_L, and the process is repeated until a balance is established. In these calculations, the average temperature of the fluid has been assumed at all times to be the arithmetic mean temperature between T_L and T_1; or between t_L and t_1, where $T_L = t_L$.

With the proper selection of the parameter k_2 and the consequent establishment of the average fluid temperature within the annular space, the receiver surface temperature can be established using Eq. (7) to

approximate a heat-transfer coefficient for the fluid film adjacent to the receiver. This receiver surface temperature, T_r, is then used in the calculation of heat losses from the receiver absorber to the surroundings.

The intervening presence of the glass jacket must be coupled into the heat balance requirements of the system. The absorber at average temperature, T_r, is losing heat by radiation to the evacuated glass jacket surrounding it to raise the temperature of the glass to some equilibrium value, T_g. In turn, the glass jacket loses heat by radiation to the environment and also by convection to the air surrounding it. When the heat entering and leaving the glass jacket are in balance, then the heat losses from the system become determinant. Therefore, the heat exchange between the receiver and glass jacket becomes

$$q_{r \rightarrow g} = \sigma A_r F_{rg}[T_r^4 - T_g^4], \tag{9}$$

and the heat loss from the glass jacket becomes

$$q_{loss} = h_g A_g[T_g - T_a] + \sigma A_g F_{g(sky)}[T_g^4 - T_{sky}^4] . \tag{10}$$

At the glass-jacket equilibrium temperature, T_g, $q_{r \rightarrow g} = q_{loss}$, and therefore, when Eqs. (9) and (10) are equated, the equilibrium value, T_g, can be established. Hence,

$$\sigma A_r F_{rg}[T_r^4 - T_g^4] = h_g A_g[T_g - T_a] + \sigma A_g F_{g(sky)}[T_g^4 - T_{sky}^4]. \tag{11}$$

The value for the sky temperature can conveniently be obtained from the relationship given by Duffie and Beckman[9]

$$T_{sky}\ (°R) = 0.09936\ (\frac{T_\infty}{1.8})^{1.5} \tag{12}$$

where T_∞ = air temperature, °R.

For air at 100°F (38°C), T_{sky} = 545°R (85°F)(29°C). The implementation of areas A_r and A_g and the calculation of the configuration factors F_{rg} and $F_{r(sky)}$, taking into account the geometry of the system and emissivities of the surfaces involved, as well as the choice of a reasonable value for h_g, the natural convection coefficient, permits the resolution of Eq. (11),

through a trial-and-error method, to calculate T_g, the glass-jacket temperature and consequently

$$Q_{loss} = h_g A_g[T_g - T_a] + \sigma A_g F_{g(sky)}[T_g^4 - T_{sky}^4] . \qquad (13)$$

Dowtherm A will be used as the heat-transfer fluid, and when the physical properties of this fluid are incorporated into the calculations described above, the results presented in Table 2 are obtained. The results of these three cases are presented graphically in Fig. 15 as collector efficiency, η, versus the difference in temperature between the receiver and ambient air (100°F)(38°C). These results show that, for small values of $t_{rec} - t_{air}$ associated with relatively low fluid outlet temperature or for small temperature increases across the tube, the efficiency is satisfactory, whereas larger temperature differences of the flowing fluid coupled with higher outlet temperatures will produce large differences of $t_{rec} - t_{air}$ and consequently lower efficiencies.

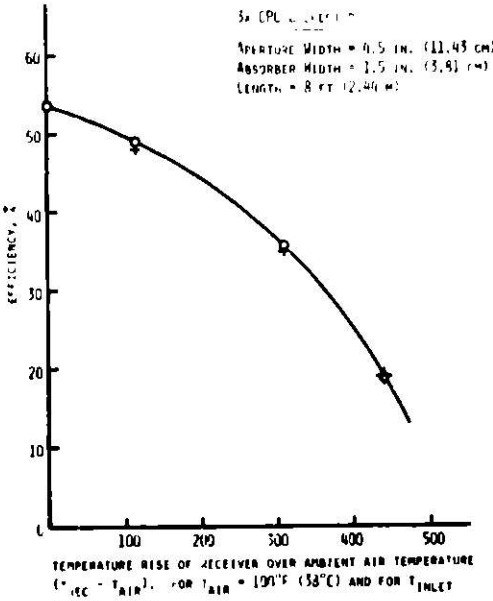

Temperature rise of receiver over ambient air temperature ($T_{rec} - T_{air}$), for T_{air} = 100°F (38°C) and for T_{inlet} near T_{exit}

Fig 15. Efficiency Predicted for CPC Collector Provided with a Glass Jacket and an Evacuated Space Surrounding Copper Currently Operating Receiver

This efficiency, η, versus $t_{rec} - t_{air}$ relationship constitutes a preliminary estimate for the thermal performance of the 3x-CPC collector under investigation. Calculations following the same basic approaches will be continued and they will be extended to involve other key variables such as the inlet and outlet temperatures of the fluid, and glass-jacket temperature with the efficiency performance of the collector.

TABLE 2. Calculated Performance of 3x CPC Collector

Aperture = 4.5 inches

Length = 8 feet

Aperture Area = $\frac{4.5}{12}$ x 8 = 3.0 square feet

Insolation = 200 Btu/hr ft^2

$Q_{entering}$ = 200 x 3 = 600 Btu/hr

Temperature of Surroundings = 100°F

$Q_{useful} + Q_{losses}$ = 0.536(600) = 322 Btu/hr

Fluid Temps., °F			Flow Rate	Average Temps., °F		Δt	Q_{loss}, Heat Loss from Glass Jacket,	Efficiency, $Q_{useful}/600$	
In	Out	Max	lb/hr	Receiver	Glass-Jacket	Receiver-Glass	Btu/hr	Assumed	Calculated
100	200	276	6.71	216	100.2	116	27	0.48	0.49
380	400	405	21.0	410	128	310	108	0.35	0.357
200	400	835	1.12	541	136	441	210	0.19	0.187

IV. COLLECTOR TESTING

A. Introduction

The performance parameters of two solar thermal CPC collectors have been measured. The first collector tested is a 10x CPC built at Argonne; this collector is an improved version of the 10x CPC described in the preceding report in this series (ANL-75-52). The second collector tested is composed of 5.3x CPCs; it was built by the Chamberlain Manufacturing Corporation.

B. Test Procedure

An efficient test procedure has been evolved which quickly establishes performance parameters for solar thermal CPC collectors. The CPC thermal performance is first characterized in nighttime or indoor measurements of heat losses to the environment from preheated receivers. The results are expressed in terms of a heat-loss coefficient

$$U_{night} = Q/A\ (T_{receiver} - T_{ambient}), \tag{14}$$

where

U_{night} = night heat-loss coefficient (Btu/hr ft^2°F or w/m^2°C)

Q = heat energy lost (Btu/hr or w)

A = input aperture area (ft^2 or m^2)

and T = temperature (°F or °C).

Experience has shown that U_{night} is an upper limit to the heat-loss coefficient that is characteristic of daytime performance. This is so because, in sunlight, the heat losses are partially suppressed by the general warming of the collector and the mirror surfaces.

The contribution to the heat loss arising from conduction losses through the back and side insulation of the CPC, denoted U_{back}, is found by repeating the heat-loss measurements with the front of the CPC covered generously with insulation.

The optical performance of the CPC is determined by measuring the energy-collection efficiency with the average receiver temperature at ambient temperature, so that the net heat loss to the environment is reduced to a second-order effect. This efficiency is given by

$$\eta_o = q/SA_1, \tag{15}$$

where

η_o optical efficiency

q = heat energy collected (Btu/hr or W)

S = total (direct beam + diffuse) insolation falling on the collector plane (Btu/ft^2 hr or W/m^2)

A_1 = input aperture area of the collector (ft^2, m^2).

In practice, it is difficult to maintain the receiver at ambient temperature, and hence, η_o is extrapolated from numerous measurements made at various temperatures near ambient. For CPCs with receivers and mirrors in the same enclosure, it is essential that the mirror surfaces also remain near ambient temperature during the optical-efficiency measurement. If light energy, absorbed by the imperfect (< 100% reflectivity) reflector material, is allowed to warm the mirrors, then the CPC will appear to have too high an optical efficiency since some of the (optically lost) energy will be transferred thermally to the receiver. To insure that this cold-mirror criterion is met, the optical efficiency is measured with the cover glasses removed. If necessary, fans are used to move ambient temperature air over the mirrors. The experimental result is then corrected for the transmission of the removed cover glasses; this is measured separately.

The performance of the CPC under test is then confirmed by the usual daytime measurements of energy-collection efficiency with covers in place. At intermediate temperatures [$T_{receiv} \approx 220°F$ (106°C)], a linear relation is found for the efficiency

$$\eta = q/SA_1 = \eta_o - U_{day}(\Delta T/S), \tag{16}$$

where

q = heat energy collected (Btu/hr, W)

S = total (direct beam + diffuse) insolation falling on collector plane (Btu/hr ft^2, W/m^2)

A_1 = input aperture area (ft^2, m^2)

η_o = optical efficiency (previously determined)

U_{day} = day heat-loss coefficient (Btu/hr ft^2 °F, W/m^2 °C)

$\Delta T = T_{receiver} - T_{ambient}$ (°F).

As described earlier, the day heat-loss coefficient is somewhat smaller than the U_{night} coefficient measured indoors, due to the general warming of the collector surfaces in sunlight.

At low receiver temperatures, the measured efficiency is found to exceed this linear prediction due to the radiative transfer of energy from the warm mirrors to the receivers, a process explicitly excluded in the determination of the optical efficiency.

C. 10x Collector Tests with Cavity Receivers

1. Construction

A second version of the 10x-CPC collector discussed previously (January-June 1975 progress report, ANL-75-52) was constructed and tested at ANL during the present reporting period to show that the optical performance could be substantially improved. The collector consisted of two 10x-CPC channels, each 4 ft (1.22 m) long and 3 ft (0.91 m) high, with a 12 in. (30.5 cm) input aperture and a 1.2 in. (3.05 cm) exit aperture. The total input aperture area was 8 ft^2 (0.744 m^2). The mirrors were sheets of 0.020 in. (0.051 cm) Kinglux metal* (measured specular reflectivity averaged over the solar spectrum ≈ 76%) fastened with small wood screws to exterior plywood ribs spaced 12 in. (30.48 cm) apart. Careful attention was paid to the fabrication of the mirror sections, and deviations from the desired mirror shape were held significantly smaller than in the case of the previous 10x collector. As before, the ends of the CPC troughs were

*Aluminum with a proprietary finish, Kingston Metal Corporation.

closed by flat Kinglux sheets to minimize the effect of the short collector length. The entire mirror structure was thermally insulated on the exterior by at least 1.5 in. (6.45 cm) of urethane foam or styrofoam sheeting. The modules were covered by a sheet of 1/8 in. (0.318 cm)-thick Plexiglass (transmission averaged over the solar spectrum ≈ 88%).

The major modification in this 10x collector concerned the receivers. For each module, a "cavity" receiver was fabricated by milling a 4 ft (1.22 m) long slot in a 3 in. (7.62 cm) diameter copper tube to match the 1.2 in. (3 cm) wide exit aperture of the CPC. Fluid-flow channels were provided by brazing 1/4 in. (0.64 cm) diameter copper tubing to the exterior of the receiver. Six such tubes ran the length of each receiver, and were connected for series flow. The interior of the 3 in. (7.62 cm) diameter receiver was painted with the same nonselective (3-M "Nextel" velvet) black paint used in the 10x collector reported in ANL-75-52 (absorptivity ≈ 90%). The receivers were nested in a bed of cast urethane foam and styrofoam sheeting with at least a 4 in. (10.16 cm) path length through the insulation from any part of the receiver to the outside aluminum framework.

For these tests, a 50-volume percent mixture of ethylene glycol and water was used as the heat-transfer fluid. The fluid was circulated via an external flow loop containing heaters and heat exchangers for controlling the temperature of the fluid at the inlet of the collector. Flow rates near 0.5 gpm were maintained, and the fluid temperatures at the inlet and outlet were monitored by immersed-platinum resistance thermometers.

2. Results

The improvements introduced through the maintenance of the proper mirror profile and the use of a cavity receiver for better absorptivity are verified by the optical-efficiency measurements. This version of the 10x-CPC collector has a measured optical efficiency $\eta_o = 0.64$, relative to the total insolation falling on the collector plane, compared to $\eta_o = 0.51$, found for the previous version of the collector.

However, the thermal performance of this version was seriously degraded. The night heat-loss coefficient was measured to be $U_{night} = 0.58$ Btu/ft^2 hr°F (3.28×10^{-4}W/cm^2°C) of which the back loss was $U_{back} = 0.27$ Btu/ft^2 hr°F (1.53×10^{-4}W/cm^2°C). This large back component, which is

almost an order of magnitude greater than the value U_{back} = 0.03 Btu/ft^2 hr°F (1.7 x 10^{-5} W/cm^2°C) measured for the previous 10x CPC collector, is attributed to the unfavorably large exterior surface area of the cavity receivers, which promotes conduction losses through the back of the collector. No significant improvement resulted from lining the interior of the urethane foam bed with shiny aluminum foil in an attempt to reduce radiative heat transfer from the receivers to the insulation.

The day heat-loss coefficient was measured to be U_{day} = 0.48 Btu/ft^2 hr°F (2.72 x 10^{-4} W/cm^2°C) at the receiver temperatures in the range 180-220°F (82-104°C). Subtracting the measured U_{back} gives U_{front} = 0.21 Btu/ft^2 hr°F (1.19 x 10^{-4} W/cm^2°C), the component due to radiation and convection losses related to the front of the collector. This value is consistent with U_{front} = 0.19 Btu/ft^2 hr°F (1.06 x 10^{-4} W/cm°C) found for the previous 10x version.

The use of a cavity receiver and the improvement in mirror profile has increased the optical efficiency of the 10x CPC test collector to 0.74 Btu/ft^2 hr°F (3.63 x 10^{-4} W/cm^2°C), an improvement of 25%. The attendant penalty in conduction losses due to increased receiver area doubled the day heat-loss coefficient. The extra insulation which would be required to reduce the conduction losses to an acceptable level would seem to make the cavity receiver an unfavorable configuration for high-temperature collectors.

D. Chamberlain Collector Tests

1. Description of Collector

A 5.3x-CPC collector was constructed for ANL by Chamberlain.* The collector consisted of nine CPC troughs 6 ft (1.83 m) long, mounted side by side in a common enclosure. Adjacent troughs shared common 6.75 in. (17.15 cm)-high aluminum extrusions of the appropriate contour to which 0.02 in. (0.051 cm) Kinglux metal sheets were fastened on each side with 3-M AF-111 adhesive to form the mirror surfaces. The ends of the troughs were closed by flat Kinglux sheets. The last mirror on each side of the collector was supported by similar aluminum extrusions, but from which one side had been machined off. The entrance aperture of each trough was 4.2 in.

*Chamberlain Manufacturing Corporation, Waterloo, Iowa.

(10.67 cm) wide, and the exit aperture was 0.8 in. (2 cm) wide. The total input aperture area of the nine troughs was 20 ft^2 (1.86 m^2).

The receivers were also 6 ft (1.83 m)-long aluminum extrusions with an integral fluid-flow channel and a profile designed to insure good optical coupling to the mirrors (Fig. 16). Milled aluminum crosspieces, spaced 15 in. (38.1 cm) apart, supported the mirrors and receivers in five places, assuring correct alignment of the separate pieces in a common assembly. The receivers were thermally isolated from the crosspieces by 0.125 in. (0.318 cm) thick Teflon mounting pads. The mirror and receiver assembly was contained in an aluminum box enclosure 86.3 in. long x 50.4 in. wide x 13.75 in. (2.18 m x 1.28 m x 34.9 cm) deep. The interior of the box was lined with 4 in. (10.16 cm) of API 520-2 urethane foam [K factor ~ 0.13 Btu-ft/ft^2 hr°F (0.0022 W/cm°C) at 75°F (24°C)]. The 2.75 in. (6.98 cm) gap between each end of the 6 ft (1.83 m) mirror-receiver assembly and the inside of the box enclosure contained manifolds which interconnected the ends of the receivers for series fluid flow through the collector.

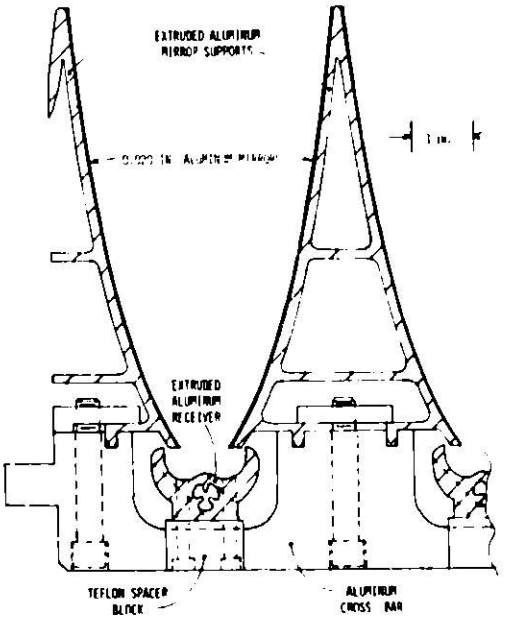

Fig. 16 Cross Section of Trapezoidal Reflectors and Receiver

The collector was covered by a sheet of 0.188 in. (0.478 cm) Clearlite* glass (transmission averaged over the solar spectrum ≈ 85%). The collector, as delivered, had the enclosed volumes containing the fluid manifolds at each end of the troughs exposed to incoming radiation under the glass. To

*Fourco Glass Company, Harding Division, Ft. Smith, Arkansas.

avoid an ambiguity in the definition of the collector input aperture, these volumes were filled with fiberglass insulation, and corresponding portions of the cover glass were masked with aluminized Mylar* on the glass exterior, thereby limiting exposure to the 20 ft^2 (1.86 m^2) input aperture area of the CPC troughs.

As in previous tests, the heat-transfer fluid was a 50-volume percent mixture of ethylene glycol and water, which was circulated at a low flow rate [$\sim$ 0.5 gpm (31.5 cc/sec)]. Immersed platinum-resistance thermometers monitored the inlet and outlet fluid temperatures.

2. Results

Indoor tests determined the night loss coefficient to be U_{night} = 0.80 Btu/ft^2 hr°F (4.54 x 10^{-4} W/cm^2°C) for average receiver temperatures of about 185°F (85°C). It was noted that the mirrors were warmer than expected in the test, averaging 145°F (63°C). With a 6 in. (15.2 cm) slab of styrofoam covering the collector, the heat-loss coefficient was U = 0.32 Btu/ft^2 hr°F (1.8 x 10^{-4} W/cm^2°C). Correcting for conduction through the slab, one obtains U_{back} $\simeq$ 0.26 Btu/ft^2 hr°F (1.47 x 10^{-4} W/cm^2°C).

Optical efficiency measurements in daylight established η_o = 0.80 for the collector with its cover glass removed. The transmission of the glass was found to be 85%, so that the optical efficiency of the assembled collector is η_o = 0.68, relative to the total insolation falling on the inclined plane of the collector.

Measurements of the collector performance at receiver temperatures in the range 180-210°F (82-99°C) show the day heat-loss coefficient to be U_{day} = 0.74 Btu/ft^2 hr°F (4.2 x 10^{-4} W/cm^2°C), given the above determined optical efficiency. As in the indoor tests, the mirrors were observed to be very warm, averaging only 40°F (22°C) lower than the receiver temperatures. The air temperature inside the enclosure was essentially the same as the mirror temperatures.

The optical performance of the Chamberlain collector is quite good, demonstrating the close conformance of the mirrors to the correct CPC shape. However, the thermal performance as characterized by the heat-loss coefficient U_{day} = 0.74 Btu/ft^2 hr°F (4.2 x 10^{-4} W/cm^2°C) is disappointing. Theoretical calculations suggest that a U_{day} in the range 0.4-0.5 Btu/ft^2 hr°F

*A product of DuPont Co., Wilmington, Delaware.

(2.3-2.8 x 10^{-4} W/cm^2°C) should be attainable. A clue to the poor thermal performance is the generally high mirror temperatures which suggest undesirable coupling of the thermal energy between the receivers and the mirrors, thereby increasing the effective area for loss mechanisms. Work in the next quarter will be directed toward reducing this coupling and removing other heat leaks as found, with indoor heat-loss tests being conducted to quantitatively measure the improvements.

V. AUXILIARY EQUIPMENT AND TEST FACILITIES

A. High-temperature Flow System

Assembly of a high-temperature flow loop for use in the testing of CPC collectors is nearly complete. Dowtherm "A" will be used as the heat-transfer fluid, with the loop operating in the temperature range 350-450°F (117-232°C). A schematic diagram of this loop is shown in Fig. 17.

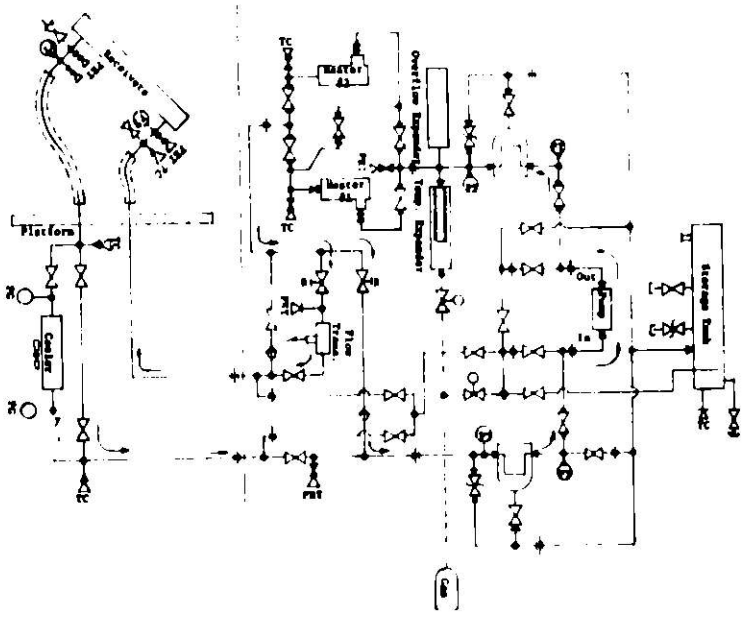

FIG. 17 HIGH-TEMPERATURE (450°F, 232°C) FLOW SYSTEM

The main components of the flow loop are turbine flow-meters, electrical heaters, in-line filters, a pump, a storage tank, and a cooler system for dumping the heat. Sufficient valves were provided to allow reversing the flow, pump draining and filling, and general flexibility of operation. Because Dowtherm "A" has a relatively high melting point (53.6°F), and is relatively viscous at low temperatures, the system will have to be maintained at an elevated temperature at all times. Trace heating of the flow lines will be used for this purpose. Dowtherm "A" also has a relatively low flash point (255°F); so to reduce concern over the potential fire hazard, the loop will be installed directly on the outdoor test stand where the collectors are to be tested and will be enclosed in a metal container.

B. Light-box Construction and Analysis

The tests on the mirror sections reported in the last semiannual progress report (ANL-75-52) were performed with a light-box apparatus located at the University of Chicago. To facilitate analysis of solar

collector sections, a light box has been constructed at ANL, and an optical system for the box has been designed. The light box and the optical system are discussed in the following paragraphs.

1. Construction

A light box has been constructed that is capable of diffusely illuminating CPCs with input apertures up to 18 in. (45.72 cm) wide. The light box, which was built of masonite sheets, is a 4 ft (121.92 cm) cube and is shown in Fig. 18; the interior of the box is coated with a highly diffusing white paint. A 2 ft^2 (0.19 m^2) opening in the side that faces the CPC under test is surrounded (inside the box) by four 36 in. (91.4 cm) fluorescent lamps, positioned in such a way that there are no direct lines of sight from the lamps to the CPC. A hole in the rear face of the box allows light reflected from the CPC to pass through to the light detector. The light box is suspended from vertical poles and can be manually raised or lowered.

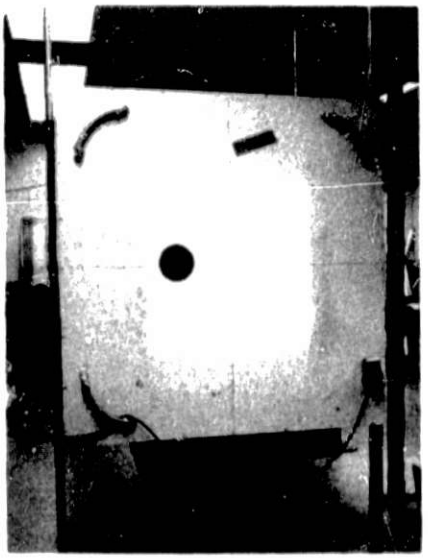

FIG. 18 LIGHT BOX

A rotatable stand is being fabricated which will support CPC modules up to 6 ft (182.9 cm) long, maintaining the long axis of the CPC vertically, and holding the CPC close to the light-box aperture. Rotation of the stand in the horizontal plane changes the angular orientation of the CPC relative to the light box, enabling the CPC reflectivity to be measured as a function of angle; provision is made for reading angles to ± 0.5°.

The light detector is a 931A photomultiplier tube. A two-stage system of lenses and apertures has been designed to couple this detector to the light box, as shown in Fig. 19. The first-stage optics consist of a 1.9 in. (4.8 cm) diameter achromatic objective, 0.020 in. (0.05 cm) diameter field stop, and a 0.4 in. (1.02 cm) diameter ocular. The entrance aperture is 1.5 in. (3.8 cm) in diameter and the full angular field of view is 0.2°. The exit pupil is matched to the active area of the photomultiplier tube. By itself, this one-stage system is suitable for investigating the optical performance of small-aperture CPCs, as well as measuring relative reflectivities of various materials.

For the investigation of large-aperture CPCs, the system described above is preceded by a second stage of optics, composed of a Fresnel-lens objective and a 1.9 in. (4.8 cm) diameter ocular. The two-stage system maintains the 0.2° full angular field of view, but increases the entrance aperture diameter to 8 in. (20.32 cm).

The necessary lenses and photomultiplier tube have been obtained, and suitable mountings are now being devised.

2. Analysis

For a solar collector, one wants to know the fraction $F(\theta)$ of the radiation incident on the aperture at angle θ that is absorbed by the absorber:

$$F(\theta) = \frac{I_{abs}}{I_{in}(\theta)} = \text{function of cover, reflector, absorptivity, geometry, mirror errors, etc.} \qquad (17)$$

Assuming that the collector aperture A is close to the light box opening L and that their areas A_A and A_L satisfy $A_A << A_L$, the illumination S_o' of the aperture is uniform and constant for the whole range of angles θ to be considered. The light box serves as a reflectometer for measuring the reflectivity $\rho_{diff \to \theta}$ for diffusely incident radiation that is reflected at an angle θ; therefore, the signal S detected by the detector D is

$$S = S_o' \rho_{diff \to \theta} . \qquad (18)$$

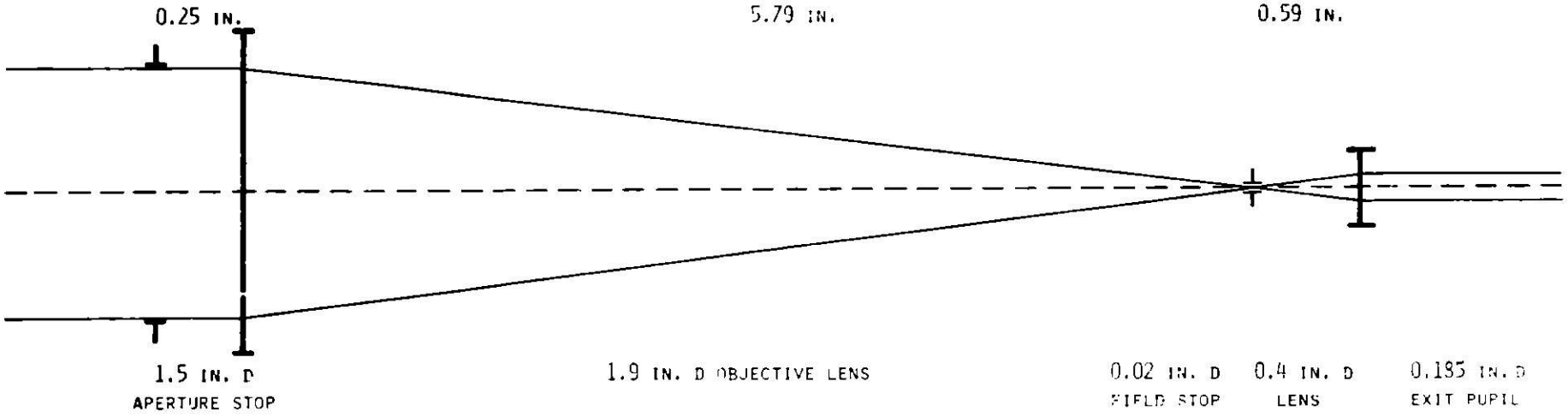

FIG. 19A FIRST-STAGE OPTICS

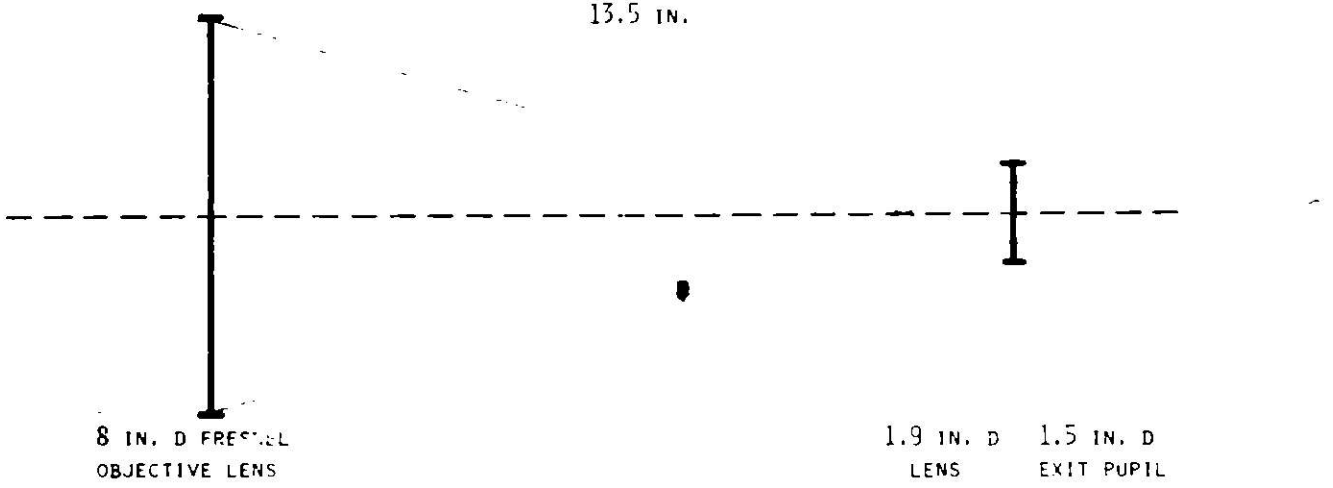

FIG. 19B SCHEMATIC OF TWO-STAGE OPTICAL SYSTEM FOR LIGHT BOX DETECTOR

Isolating the cos θ factor from the illumination, this can be rewritten as

$$S = S_o \cos\theta \, \rho_{\theta \to \text{diff}} \tag{19}$$

where S_o is another constant and $\rho_{\theta \to \text{diff}}$ is the total diffuse reflectivity for radiation incident at θ. (S_o is constant as long as the light-box power output, aperture of collector, and the detector are not changed.) To relate $\rho_{\theta \to \text{diff}}$ to the properties of the CPC, let

$$f(\theta) = \text{angular acceptance characteristic;} \tag{20}$$

$$= \frac{\text{radiation reaching absorber, if reflector has } \rho_R = 1}{\text{radiation incident on aperture at angle } \theta}$$

ρ_a = reflectivity of absorber;

$\bar{\tau}_R$ = effective average transmissivity of CPC averaged over all incident radiation which can reach absorber;

$\tau_R(\theta)$ = effective transmissivity of CPC for radiation incident at angle θ which can reach absorber;

$\tau_{R\ \text{out}}(\theta)$ = effective "reflectivity" of CPC for radiation which cannot reach absorber.

With these definitions, one can write $\rho_{\theta \to \text{diff}}$ as

$$\rho_{\theta \to \text{diff}} = \underbrace{f(\theta)\ \tau_R(\theta)\ \rho_a \bar{\tau}_R}_{\left[\begin{array}{l}\text{contribution from}\\ \text{radiation which}\\ \text{reaches absorber.}\end{array}\right]} + \underbrace{[1 - f(\theta)]\ \tau_{R\ \text{out}}(\theta)}_{\left[\begin{array}{l}\text{contribution from}\\ \text{radiation which does}\\ \underline{\text{not}}\ \text{reach absorber.}\end{array}\right]} . \tag{21}$$

Indicating the dependence of the signal S on incidence angle θ and on absorber reflectivity ρ_a explicitly, one can rewrite Eq. (19) as

$$S(\theta, S_a) = S_o \cos\theta \{f(\theta)\ \tau_R(\theta)\ \rho_a \bar{\tau}_R + [1 - f(\theta)]\ \tau_{R\ \text{out}}(\theta)\} . \tag{22}$$

Let us return to Eq. (17) for the quantity we really want to know,

$$F(\theta) = \frac{I_{abs}}{I_{in}(\theta)}$$

and express it in terms of $f(\theta)$, $\bar{\tau}_R$, $\tau_R(\theta)$, ρ_a, and $\tau_{R\ out}(\theta)$ as

$$F(\theta) = f(\theta)\ \tau_R(\theta)\ (1 - \rho_a). \tag{23}$$

This is not measured by the light box. However, one can come close to extracting the desired information by measuring $S(\theta,\rho_a)$ both with a black ($\rho_a \simeq 0$) absorber and with a white ($\rho_a \simeq 1$) absorber. When these two measurements are subtracted from each other, the term $[1 - f(\theta)]\ \tau_{R\ out}(\theta)$ drops out of Eq. (22) and one obtains

$$f(\theta)\ \tau_R(\theta)\ \bar{\tau}_R = \frac{S(\theta,\rho_a = 1) - S(\theta,\rho_a = 0)}{S_o \cos\theta} \tag{24}$$

The value of the constant S_o can be determined by measuring the signal

$$S(\theta,\ \rho,\ \text{flat}) = S_o \cos\theta\ \rho \tag{25}$$

from a simple flat reflector of known reflectivity ρ. [This is a special case of a CPC with unit concentration, $\bar{\tau}_R = \tau_R(\theta) = 1$, $f(\theta) = 1$, see Eq. (21).] Note that the reflectivity of any material can be measured with the light box, once S_o has been determined by a single normalizing measurement with a material of known reflectivitiy ρ.

For a highly truncated CPC (such as the ones to be used in practice), the average number of reflections $\langle n(\theta)\rangle$ does not vary significantly with angles (less than ± 10%); therefore, the transmissivity $\tau_R(\theta)$ is nearly independent of θ, and one can rewrite Eq. (24) as

$$f(\theta)\ (\bar{\tau}_R)^2 = \frac{S(\theta,\ \rho_a = 1) - S(\theta,\ \rho_a = 0)}{S_o \cos\theta} \tag{26}$$

Since the mirror error Δ (angular deviation of mirror shape from correct slope) is small compared to the acceptance angle of the CPC, $f(\theta) = 1$ for values of θ within the acceptance angle and Eq. (26) provides a direct measure of the desired transmission factor $\bar{\tau}_R$.

C. Computer-controller Data System

A data-acquisition system capable of controlling several solar-collector tests simultaneously is under construction. The system is based on a Data General NOVA 2/10 minicomputer and uses the industry standard CAMAC to

interface the computer to test instruments and control systems. A Texas Instruments Silent 700 ASR terminal with dual magnetic-tape cassettes functions as a data logger, as well as the operator's console. A high degree of system flexibility is assured by the function module organization of CAMAC and the large body of software available for the NOVA-line of computers.

All the major hardware components have arrived and have been interfaced with one another. Numerous diagnostic programs have shown the NOVA-to-CAMAC interface to be functioning reliably. A number of modifications made to the Silent 700 terminal and its associated electronic interface have rendered it fully compatible with both the NOVA hardware and the NOVA software. As a consequence, unmodified Data General computer programs as well as data is stored and read from the tape cassettes.

The primary analog input device for the system is a Systron-Donner 7110A Digital Voltmeter (DVM), with ± 0.005% accuracy and resolution to 1 μV. Several standard CAMAC digital input/output modules have been modified to give complete computer control and readout of the DVM. CAMAC relay multiplexer modules provide the capability to switch the DVM among various analog devices such as temperature and insolation transducers. Digital inputs from devices such as flow meters will be monitored directly by CAMAC digital input modules.

The capability to control a solar-collector test is provided by a CAMAC digital-to-analog converter module which gives analog reference signals for such systems as the flow system temperature controller. In addition, several CAMAC digital output modules give switching capability to turn pumps on and off, open and close valves, etc.

The CAMAC modules described above have been tested in a closed loop by connecting the digital-to-analog converter through the multiplexer to the DVM, which allows the computer to produce an analog signal, select it as the input to the DVM, and read it back for comparison.

Software for the data-acquisition system is being developed in as modular fashion as is possible. A software module has been written and debugged which allows Data General's interactive BASIC language to access the CAMAC interface as well as several NOVA devices (such as the real time clock) to which BASIC did not originally have access. This development

permits one to quickly write and execute programs in an easily-learned language for the monitoring and controlling of single solar-collector tests.

Work is in progress to specify software modules which will maintain the CAMAC interface under Data General's Real Time Operating System (RTOS). This level of support will permit the development of real-time programs for conducting tests of several solar collectors simultaneously and independently, using the well-known, high-level FORTRAN language.

VI. ANALYSIS OF COLLECTOR OPTICS

The design and analysis of nonfocusing concentrators for flat absorbers and vertical-fin absorbers have been reported in previous ANL semi-annual reports and in the open literature. This section presents further analyses required for some advanced applications of the collector concept.

The use of an evacuated glass envelope around an absorber to reduce heat losses imposes a constraint on the optics of the system because light reflected from the mirrors must pass through the glass surface before being absorbed. An analysis of the optical aberrations is reported in Section VI.A.

Section VI.B describes the design of concentrators for cylindrical absorbers (such as tubes). Advanced solar collector designs using tube absorbers are in progress, and the results of this analysis are directly applicable. Section VI.C describes work done on the analysis of nonimaging concentrators for use as second stage of primary line-focus concentrators. Section VI.D discusses mirror modifications that may be used to accommodate a gap between mirror and absorber required by an evacuated glass tube.

A. Optics of Glass Tubes

To reduce heat losses in solar-thermal collectors, it may be desirable to place the absorber inside an evacuated glass tube. The effects that refraction in the glass tube might have on the optics of a solar concentrator can, of course, be determined by detailed ray tracing. However, a much simpler method is provided by the relationship between rotational symmetry and angular momentum conservation.[10]

For this purpose, it is convenient to invoke the Hamiltonian theory of geometrical optics[11] according to which a light ray propagating in the direction $\hat{s}$ in a medium with index of refraction n is associated with a canonical momentum

$$\vec{p} = n\hat{s}. \tag{27}$$

If a ray has momentum $\vec{p}$ at a point $\vec{r}$, then its angular momentum relative to another point $\vec{r}$ is

$$\vec{\ell} = (\vec{r} - \vec{r}_o) \times \vec{p} \ . \tag{28}$$

In a system with rotational symmetry, the corresponding angular momentum is constant for all points along a given light ray. For example, if a system is rotationally symmetric about the z axis, the conserved angular momentum is

$$\ell_z = nr\sqrt{1 - s_z^2} \tag{29}$$

where r is the impact parameter of the light ray (= shortest distance between light ray and z-axis). For the glass tube shown in Fig. 20, conservation of angular momentum implies that the impact parameters r_o, r_1 and r_2 of the light ray R outside the tube, in the tube wall and inside the tube, respectively, are related by

$$r_o = nr_1 = r_2 \tag{30}$$

if R is in the plane,[12] and by

$$r_o\sqrt{1 - s_z^2} = nr_1\sqrt{1 - (s_z/n)^2} = r_2\sqrt{1 - s_z^2} \tag{31}$$

if R is nonplanar with z component s_z. If R would have been tangent to the absorber tube in the absence of the glass envelope, it would also be tangent to this absorber (at a different point) after passing through the envelope. Therefore, the concentration value of the whole system is not changed by

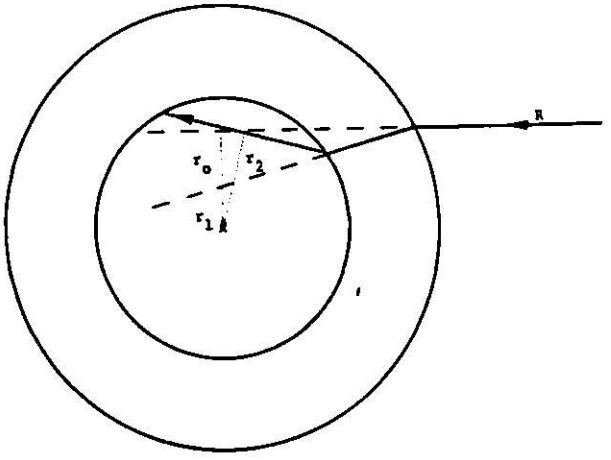

FIG. 20 REFRACTION OF LIGHT RAY BY GLASS TUBE

the addition of an envelope. This result holds both for planar and for nonplanar rays, and is independent of the index of refraction or the size of the tube.

The local intensity distribution at a particular point on the absorber may be changed somewhat by refraction, in a way which depends on the distribution of radiation incident on the envelope. However, in the important special case of uniform illumination, not even the intensity distribution on the absorber is changed by the glass envelope. The laws of radiation concentration[13,14] imply that the illumination of the absorber is isotropic in any system which achieves the maximum concentration value

$$C = \begin{cases} 1/\sin\theta \text{ for 2-dimensional concentrators} \\ (1/\sin\theta)^2 \text{ for 3-dimensional concentrators} \end{cases} \tag{32}$$

where θ is the angular half-width of the radiation source (assuming the source is uniform over all angles $|\theta'| < \theta$; this is very well satisfied by the sun, with $\theta_s = 1/4°$). The closer the concentration is to the limit C of Eq. (32), the more uniform is the illumination of the absorber and the less it is changed by the addition of a glass envelope.

Analogous results hold, of course, for spherical arrangements.

B. Design of Second-stage Concentrators

Second-stage concentrators collect and further concentrate radiation coming from a primary concentrator such as Fresnel lens, parabolic trough or Fresnel mirror as shown in Fig. 21. The acceptance half angle ϕ of the second stage should be at least equal to the rim angle of the first stage (about 30° in some typical line-focus systems). The highest possible concentration value Eq. (32) of the second stage is $1/\sin\phi$ for line focus and $(1/\sin\phi)^2$ for point-focus systems.

For a sample analysis, the Fixed-Mirror-Moving-Receiver collector of General Atomic has been evaluated and a comparison is made among three modes of operation: (1) without a second stage, (2) with a V-trough second stage, and (3) with a CPC second-stage concentrator. The conclusions reached are also applicable to other line-focus systems. (The second stages analyzed for the General Atomic Collector are shown in Fig. 22.) Under normal operating conditions, a V-trough will increase the system

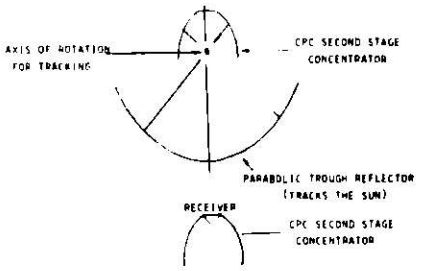

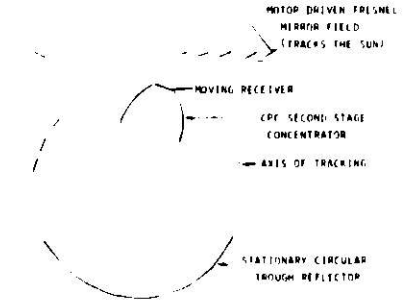

FIG. 21 THREE MEDIUM CONCENTRATORS USING THE CPC AS A SECONDARY STAGE

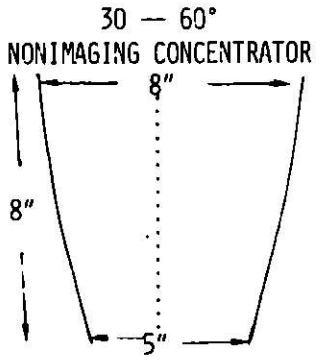

CPC TYPE SECOND STAGE DESIGNED FOR AN ENTRANCE ANGLE OF 30° AN INCIDENCE ANGLE ON THE ABSORBER OF 60° AS SECOND STAGE.

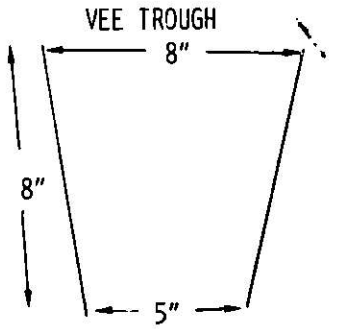

V-TROUGH - SECOND STAGE HAS MORE REFLECTION LOSSES, REJECTS SOME RAYS, AND DOES NOT RESTRICT ANGLE ONTO ABSORBER.

FIG. 22 SECOND STAGE CONCENTRATOR

output by a factor 1.06, and a CPC by a factor 1.1 over a system without second stage. (These numbers represent estimates based on reasonable operating conditions.) Since the second stage is only a small component of the overall system, the incremental cost of the unit is small and its use is recommended.

The design principle is very flexible and several design variations can easily be incorporated, for example, restricted angles of incidence on the absorber (at a slight decrease in concentration), arbitrary absorber profiles, and reflectors that surround the absorber (to reduce or eliminate losses through insulation in back of the absorber). Beyond the obvious advantages of higher concentration (or equivalently lower tracking and mirror accuracy requirements), a CPC distributes the radiation on the absorber more uniformly. It can also be used to suppress convection.

C. Analysis of Non-focusing Concentrators for Tube Absorbers

Recently, Winston and Hinterberger[14] have shown that in two dimensions, radiation with $|\theta| < \theta_{max}$ can be concentrated by a factor $1/\sin \theta_{max}$ onto an absorber of arbitrary (convex) cross section. However, they did not calculate the required reflector shape explicitly. In fact, until now the reflector shape has been known explicitly only for absorbers consisting entirely of straight sections as in the examples in Fig. 23, where the reflector is formed by appropriate parabolic and circular sections (for details see Ref. 15).

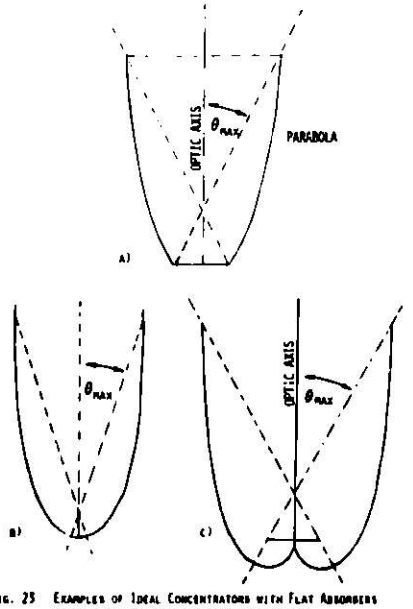

FIG. 23 EXAMPLES OF IDEAL CONCENTRATORS WITH FLAT ABSORBERS
A) COMPOUND PARABOLIC CONCENTRATOR (CPC)
B) CONCENTRATOR FOR VERTICAL FIN
C) CONCENTRATOR FOR HORIZONTAL FIN

The reflector shape is determined by a first-order differential equation. As usual, with such equations, considerable simplification can result from a suitable choice of variables. It is convenient to describe the absorber by polar coordinates (r,θ) and to characterize any point B on the reflector by its distance $\rho = \overline{BC}$ from the point C at which the tangent CB touches the absorber. The angle θ is measured from the negative y-axis as shown in Fig. 24. The general solution is described in Ref. 15.

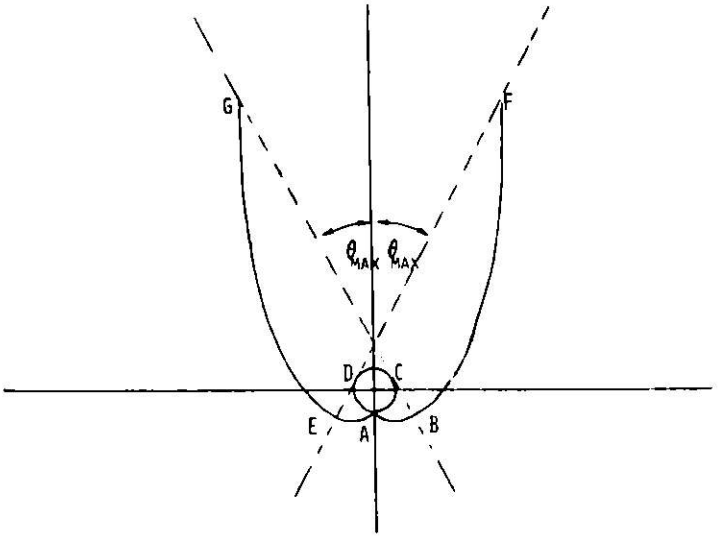

FIG. 24 IDEAL CONCENTRATOR FOR TUBE ABSORBER

For the special case of a circular absorber (i.e., a tube), the explicit solution for the reflector shape is

$$\rho = a\theta \text{ for } |\theta| \leq \theta_{max} + \frac{\pi}{2} \tag{33}$$

and

$$\rho = a\,\frac{\theta + \theta_{max} + \frac{\pi}{2} - \cos(\theta - \theta_{max})}{1 + \sin(\theta - \theta_{max})} \text{ for } \theta_{max} + \frac{\pi}{2} \leq |\theta| \leq \frac{3\pi}{2} - \theta_{max} \tag{34}$$

where a is the tube radius. An example with $\theta_{max} = 30°$ (concentration = 2) is shown in Fig. 25. In most practical applications, a large portion of the reflector at the inlet aperture end can be cut off with little decrease in concentration.[7,16]

Because of absorption at the reflector surface, only a fraction τ of the radiation incident on the aperture will be transmitted to the absorber. Since in concentrators of this type the number of reflections varies both

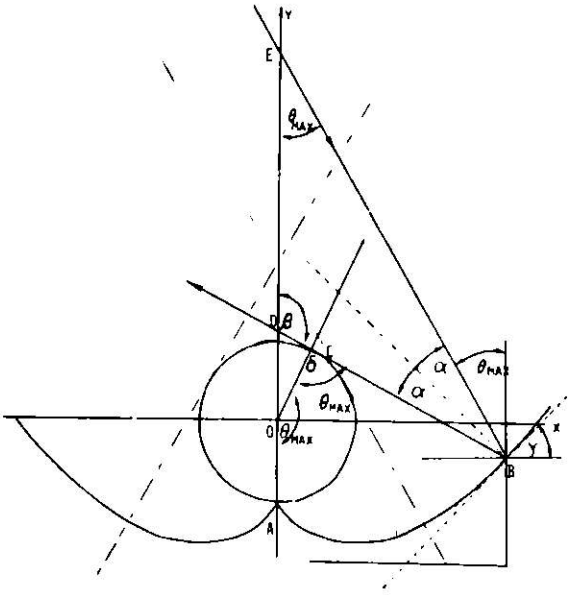

FIG. 25 COORDINATES AND PARAMETERS USED FOR DESCRIBING ABSORBER AND REFLECTOR

with angle and with point of incidence, an exact calculation of τ is difficult. But in most cases, a good approximation is provided by the formula

$$\tau = \rho^{\langle n \rangle}$$

where ρ is the reflectivity of the reflector and $\langle n \rangle$ is the average number of reflections. The value of $\langle n \rangle$ can be calculated either analytically[17] or by ray tracing. For low concentrations (two to ten), $\langle n \rangle$ ranges from about 1 to 1.5 and it increases logarithmically with concentration. For the convolute portion of Fig. 25, the formula for the average number of reflections is particularly simple. If the radiation incident on the aperture FG of Fig. 25 is uniformly distributed over all angles $|\theta| < \theta_{max}$, then it will be isotropic when it reaches the surface BCDE. On its passage from surface BCDE to the absorber tube ACD itself, this radiation undergoes

$$\langle n \rangle_{convolute} = \left(\theta_{max} + \frac{\pi}{2}\right)^2 \Big/ 4\pi \tag{35}$$

reflections at the convolute reflector section EAB, and is attenuated by a factor

$$\tau = \rho^{(\theta_a + \pi/2)^2/4\pi} . \tag{36}$$

In particular, a cusp with unit concentration (i.e., aperture width = tube circumference) corresponds to $\theta_a = \pi/2$; hence $\langle n \rangle = \pi/4$ and the transmission factor is

$$\tau = \rho^{\pi/4} \quad . \tag{37}$$

D. Optical and Thermal Design Considerations

In the compound parabolic concentrator (CPC), as well as in any other concentrator with maximal concentration, the reflector must extend to the edge of the exit aperture or absorber surface. Thermal considerations, on the other hand, necessitate a gap between absorber and reflector in order to minimize conductive heat losses as shown in Fig. 26. The potential cooling-fin effect is particularly serious if the reflector is made of aluminum. Clearly, a compromise is called for between absorber and thermal performance. In this section, the effect of a gap between absorber and reflector is studied systematically.

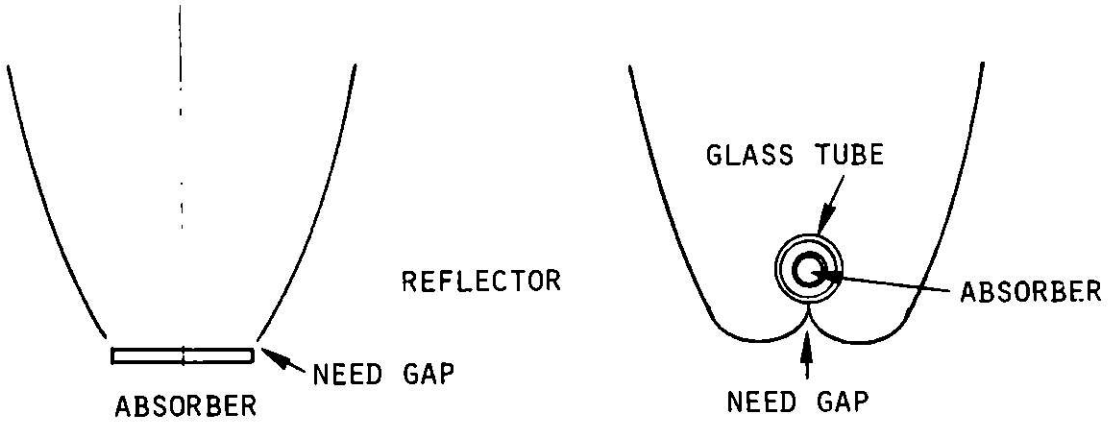

FIG. 26 OPTICAL AND THERMAL DESIGN PROBLEMS

Three solutions are possible without any alteration in the basic reflector shape:

(i) Unchanged reflector plus cavity absorber as shown in Fig. 27B.

(ii) Unchanged reflector plus truncated absorber as shown in Fig. 27A.

(iii) The truncate reflector near the absorber, leave the absorber unchanged as shown in Fig. 27D.

The optical effects can be evaluated analytically and stated as simple expressions involving radiation shape factors. Solution (i) is free from optical losses, but entails practical thermal or mechanical problems (increased convective and conductive losses due to the larger absorber area; also, solution (i) is an impractical shape for an evacuated glass tube). Since a cavity is undesirable, solution (iii), with optical losses of approximately 0.3 g/a, is preferable to solution (ii), with optical losses equal to g/a, where g/a is the ratio of gap width to absorber width. Since values of g/a $\lesssim$ 0.1 can easily be obtained, the optical losses can be kept below 3%.

Altering the reflector shape, for example, by a parallel displacement of the two reflector sides (Fig. 27C), is optically inferior to solution (iii). These conclusions hold not only for the CPC, but also for other ideal concentrators, e.g., concentrators with restricted exit angles, with other absorber shapes, and with finite sources (second-stage concentrators).

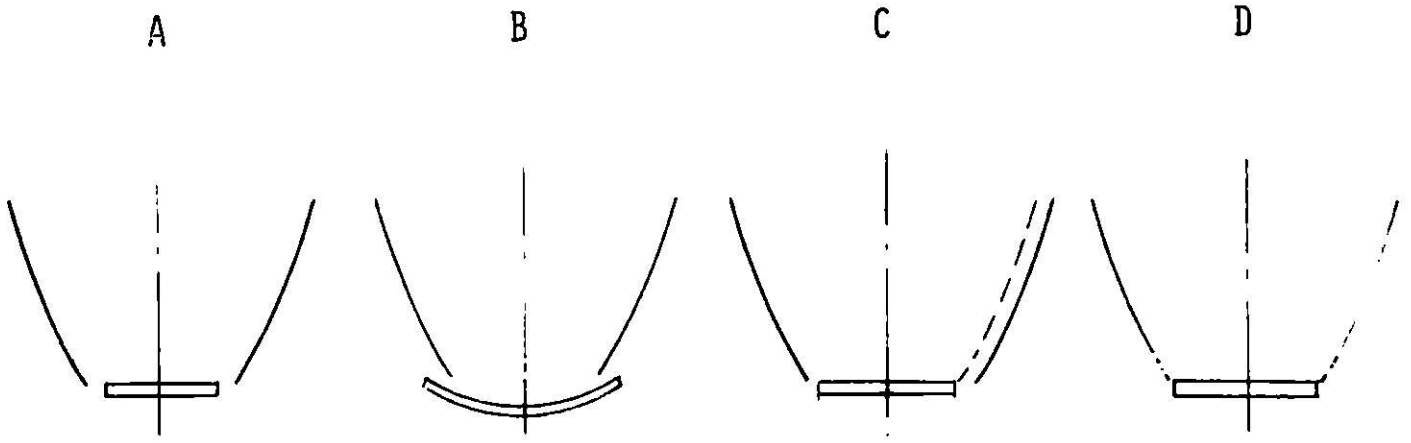

FIG. 27 SOLUTIONS ILLUSTRATED FOR FLAT RECEIVER CPC

VII. SUBCONTRACT RESULTS

A. Chamberlain Manufacturing Corporation

The subcontract to Chamberlain Mfg. Corp. was to fabricate two collectors using the CPC concept. Each collector was to be 20 ft^2 (1.86 m^2) in aperture area, complete with an enclosure bar, cover glass, fluid-flow channels, and insulation. The unit was delivered and has been tested at Argonne National Laboratory; the results of the testing are reported in Section IV-D.

B. American Science and Engineering, Inc.

A contract similar to that awarded to Chamberlain Mfg. Corp. was issued to American Science and Engineering, Inc. (AS&E) for fabrication of two panels each with a 20 ft^2 (1.86 m^2) aperture area. The method of fabrication chosen by AS&E was to roll-form the reflective aluminum sheets into the CPC bars. Because considerable trouble was experienced in producing acceptable parts, a new fabrication technique has been devised. This technique consists of pressing the sheets to the proper shape and then bonding them to ribs. The testing of the AS&E collector will be reported in a future ANL quarterly progress report after receipt of the collector panels.

C. Mobil Tyco Solar Energy Corp.

The subcontract to Mobil Tyco Solar Energy Corp. was to perform an evaluation of the potential for coupling a CPC to photovoltaic cells. The final report of this study has been released to the NTIS, Springfield, Va., for reprinting. The Mobil's executive summary of the report is reproduced below.

"A brief (7 weeks) but intensive program was conducted to determine the potential of using silicon solar cells in Compound Parabolic Concentrators (CPC) as a means for effecting considerable reduction in the cost of photovoltaic systems.

"The specific tasks which were performed included:

"1. Determination of the performance characteristics of state-of-the-art (i.e., Czochralski N on P) silicon solar cells as a function of concentration ratio (up to 10 times) and temperature (20-100°C).

"2. Maximization of solar cell performance under concentration and at elevated temperatures, including electrode grid design, junction depth, and antireflection coating.

"3. Analysis of CPC/solar cell performance as a function of concentration ratio and degree of truncation (and hence of acceptance angle), including determination of the energy distribution on the cells to provide design guidance for the location of the grid structure.

"4. Analysis of the cost effectiveness of the CPC/silicon solar cell system.

"The major findings in each of these areas were as follows:

"1. Silicon solar cells can readily be designed to increase in efficiency with concentration up to 10 suns. This result is expected from theory so long as the series resistance can be made adequately low. Simple improvements in grid structure permit the attainment of the requisite value in series resistance.

"2. The specific cell parameters required to achieve enhanced efficiency with increasing concentration have been defined, and these are readily attainable with minimum modification of standard solar cell fabrication techniques.

"3. Based on a novel computer program which we developed, we have determined the energy distribution on the exit slit of a CPC as a function of concentration ratio, degree of truncation, and direction of incident light. The results are both novel and unexpected. They have two important consequences, namely provision of accurate design data for optimizing total energy received on the exit slit over a period of time, and determination of energy distribution data necessary to optimize the design of the electrode structure.

"4. The cost of a CPC/solar cell system was determined as a function of concentration ratio, taking into account specific materials of construction, means for maintaining the cells at reasonable operating temperatures, and construction costs of the CPC array. Cost calculations were performed based on projected silicon solar cell devices down to $12/sq. ft. It was determined that the total cost of a CPC/solar cell system will be between 4 and 5

> times lower than for flat plate silicon cell arrays. This lowest cost occurs at a concentration ratio of between 8 and 10 times, a range of values consistent with achieving good total energy collection with a minimum of positional adjustment throughout the year.

"In the brief time available for this study, it has not been possible to carry out the very detailed work necessary for optimization of this clearly extremely potent approach to low cost photovoltaic systems. For example, little or no consideration has been given to the fact that the CPC/solar cell system at 8-10 times concentration ratio, provides valuable low grade heat output as well as electricity. The ratio of energy output as low grade heat to that as electricity is close to ideal for use by domestic residences. The overall cost effectiveness of this system is much improved if this is taken into account.

"Despite the inevitable shortcomings of such a brief effort, we believe that the basic validity of the CPC/solar cell system has been amply demonstrated, and that further work in its development will lead rapidly to low cost photovoltaic systems which consume a relative minimum of silicon, and which will continue to benefit from lower silicon solar cell prices as they become available.

"We recommend that urgent consideration be given to continuing and expanding this work with the objective of constructing an operating prototype system which can be evaluated outdoors over an extended period. A first goal of such a program might be a combination photovoltaic and thermal system, the electrical output being sufficient to operate all of the pumps, fans, controls, etc., required to provide heating, hot water and air conditioning for a particular dwelling. The second phase would be to construct a completely energy self-sufficient dwelling.

"Finally, it should be noted that the EFP process for making silicon ribbon has the prospect of providing low cost solar cells of a geometry ideal for use in CPC/solar cell systems. Parallel programs in CPC/solar cell systems and in EFG silicon solar cell development will provide the basis for low cost photovoltaic systems of general applicability, and of particular value for providing combined electrical and thermal outputs for domestic residences."

The positive results of the study have been an additional stimulus to ANL to expand the development of the concept from one with strictly photothermal applications to one that also includes photovoltaic applications. A program plan to develop CPCs for photovoltaic applications has been submitted to ERDA.

D. Spectrolab, Inc.

The contract to Spectrolab was to evaluate the CPC-type collector for use as the second stage for line-focus-type primary concentrators for photovoltaic applications. The study concluded that "the two-element concentrator is superior to any single element concentrator for use in photovoltaic systems." Spectrolab and Arizona State University, on the basis of this study, then requested and received funding from ERDA to build and test a second-stage concentrator for a photovoltaic application.

E. Arthur D. Little, Inc.

The A. D. Little subcontract was to perform a goals study for the technical development and economic evaluation of the CPC concept for solar collector applications. The objective of this study was to determine the technical applicability and the economic viability of the compound parabolic concentrator concept for all solar energy applications except large central power plants. The conclusions and recommendations from the study are presented below, and the entire report may be ordered from NTIS in Springfield, Va.

"Conclusions

"1. The CPC concept is not competitive when compared with other flat plate solar collectors for use in low temperature heating and domestic hot water applications. This is because the temperature requirements for these applications are modest (100-150°F) and can easily be met by low cost flat plate collectors that are often used to share the heating load with conventional gas or oil fired heating systems.

"2. The potential applications for the CPC are in systems where the working temperature is greater than about 190°F. The CPC is particularly attractive for use with solar hot water systems that use an insulated water tank for solar thermal storage in the 150-200°F range. Such high temperatures can be used to facilitate the load management of conventional hot water

heating systems. Space cooling with lithium bromide - water absorption units operating at temperatures in excess of about 190°F are particularly attractive when used in conjunction with high temperature storage.

"3. The CPC is particularly attractive for on-site power generation concepts that require temperature in excess of 200°F (for example the Rankine-cycle engine). The major application for such on-site power generation systems is water pumping at remote locations where power from central power stations is not available. Although technically feasible, the potential market for Rankine-cycle power systems is uncertain at this time because commercial units are not available, they are expensive, and competition is from electrical power.

"4. The principal competition for the CPC are evacuated selective surface collectors that can be manufactured on highly automated production lines. The use of CPC reflectors for modest augmentation (up to 3 X) of evacuated selective receivers offers reduction in the predicted cost of delivered energy when compared with non-augmented evacuated selective surface collectors.

"5. The CPC concept is attractive for moderate concentration of energy for photovoltaic applications. However, the CPC is limited to concentration ratios of approximately 10 X and, at this concentration, requires frequent adjustments of the pointing axis. The competition is with high concentration focusing devices that have concentrations greater than about 30 X. Consideration should be given to the use of a CPC as a terminal coupling element in focusing optical systems.

"Recommendations

"The following recommendations are presented in order of priority for early implementation.

"1. The performance of CPC units should be measured in terms of the average daily, average monthly, and average yearly heat absorbed. These data along with the cost per unit area and expected lifetime are the important parameters required by system designers.

"2. The feasibility should be investigated for incorporating CPC collectors into high temperature heating and cooling systems. Systems analysis must be made for each application to determine the optimum arrangement

of components, the amounts of conventional and solar energy to be used, and the savings to be expected over the lifetime of the installed system.

"3. The applicability of CPC collectors to Rankine-cycle power generation systems, particularly in sizes up to 100 HP should be studied.

"4. Further investigations should be made into the feasibility of using an evacuated-selective surface collector as the receiver for the CPC with a concentration ratio of about 3 X. Fabrication optimization studies should include this system and units should be assembled for evaluation.

"5. A demonstration program should be defined to establish the credibility of the CPC system for use by the HVAC industry. HVAC designers will not specify solar devices until they are proven, commercially available, and are competitive with other systems."

The recommendations of A. D. Little (numbers 1-5) have heavily influenced the direction of the present program as described in Sections II through VI of this report.

F. Bechtel Corporation

The objectives of the Bechtel Contract were identical to those for the Arthur D. Little contract discussed above. The conclusions substantially supported those previously stated, and are quoted below. The entire report is available from NTIS at Springfield, Va.

"● The goals study should be continued in significantly greater depth to direct CPC solar collector development.

"● Residential and commercial solar applications seem to offer greater near-term potential than do industrial process heat applications.

"● In particular, absorption air conditioning, Rankine engine driven generators and air conditioning compressors, and photovoltaic devices for residential and commercial space conditioning applications seem to be compatible systems with CPC solar collectors. CPC collector development should be coordinated with the development of the principal ancillary devices of these systems.

"● Design and manufacturing methods required for the economic mass production of CPC solar collectors should be investigated. The collectors must be durable, efficient and of low cost.

"• A 20-year design lifetime appears to be a minimum requirement for solar collectors.

"• The economics and market potential of CPC solar collectors depends on local climatological factors, specific applications, competing fuel costs, and acceptance by the building industry. All of these factors should be investigated further to provide marketing goals.

"• To promote market acceptance of the CPC collectors, the panels should be integrable into building structures and should satisfy applicable building codes.

"• Once the market potential is determined, a plan should be developed for the dissemination of technical and economic data to potential fabricators, distributors, dealers, builders and consumers."

REFERENCES

1. R. B. Pettit and R. R. Sowell, *J. Vac. Sci. Technol.*, 13 (2), 596 (1976).

2. *Goals Study for Technical Development and Economic Evaluation of the Compound Parabolic Concentrator Concept for Solar Energy Collector Applications*, Arthur D. Little, Inc., ANL-K-75-3190-1 (July 1975). (Available from NTIS.)

3. *Goal Study for the Technical and Economic Evaluation of the Compound Parabolic Concentrator (CPC) Concept Applied to Solar, Thermal, and Photovoltaic Collectors*, Bechtel Corporation, ANL-K-75-3192-1 (June 1975). (Available from NTIS.)

4. *Photovoltaic Engineering Services Pertinent to Solar Energy Conversion*, Mobile-Tyco Solar Energy Corporation ANL-K-75-3171-1 (June 1975). (Available from NTIS.)

5. R. Giugler et al., *Compound Parabolic Concentrators for Solar-Thermal Power*, Argonne National Laboratory Semiannual Report for January-June 1975, ANL-75-52.

6. J. R. Williams, *Solar Energy and Technology Applications*, Ann Arbor Science Publishers, Inc., Ann Arbor, Michigan (1974).

7. A. Kabl, *Optical and Thermal Properties of Compound Parabolic Concentrators*, Argonne National Laboratory Report SOL 75-01 (1975); Solar Energy, 18, 497 (1976).

8. M. Jakob, *Heat Transfer*, 1, John Wiley, New York, 544 (1949).

9. J. A. Duffie and W. A. Beckman, *Solar Energy Thermal Processes*, John Wiley, New York, 76 (1974).

10. See for example, *The Feynman Lectures on Physics*, R. P. Feynman, R. B. Leighton, and M. Sands, Addison and Wesley Publishing Company, Reading, MA (1964).

11. See for example, *Mathematical Theory of Optics*, R. K. Steunenberg, University of California Press, Berkeley and Los Angeles (1964).

12. For planar rays, this result was derived by ray tracing by A. D. Stokes, *Optics of Circular Glass Tubes*, J. Opt. Soc. Amer. 57, 1100 (1967).

13. R. Winston, *Light Collection Within the Framework of Geometrical Optics*, J. Opt. Soc. Amer. 60, 245 (1970).

14. R. Winston and H. Hinterberger, *Principles of Cylindrical Concentrators for Solar Energy*, Solar Energy 17, 255 (1975).

REFERENCES (Contd)

15. A. Rabl, *Solar Concentrators with Maximal Concentration for Cylindrical Absorbers*, Applied Optics 15, 1871 (1976).

16. A. Rabl, *Comparison of Solar Concentrators*, Argonne National Laboratory Report SOL 75-02 (1975); Solar Energy, 18, 93 (1977).

17. A. Rabl, *Radiation Transfer Through Specular Passages*, Argonne National Laboratory Report SOL 75-03 (May 1975); Int. J. Heat and Mass Trans. 20, 323 (1977).

18. G. Thodos, *Predicted Heat Transfer Performance of an Evacuated Glass-Jacketed CPC Receiver: Countercurrent Flow Design*, Argonne National Laboratory Report ANL-76-67 (May 1976).

Distribution of ANL-76-71

Internal:

J. P. Ackerman
J. W. Allen
J. Barghusen
J. E. Battles
E. C. Berrill
L. Burris
F. A. Cafasso
A. A. Chilenskas
P. Cunningham
J. G. Eberhart
R. Elliott
W. Frost
E. C. Gay
A. Gorski
F. Hornstra
R. O. Ivins
A. A. Jonke
R. Kampwirth
G. M. Kesser
R. W. Kessie
D. Knox
V. M. Kolba
M. L. Kyle
W. Lark
S. Lawroski
N. Levitz
L. Link
A. E. Martin
J. H. Martin
R. G. Matlock
A. Melton
W. E. Miller
F. Mrazek
K. M. Myles
P. A. Nelson
E. G. Pewitt
E. R. Proud
A. Rabl
K. Reed
M. F. Roche
J. Royal
R. Rush
W. W. Schertz (200)
V. Sevcik
H. Shimotake
R. K. Steunenberg
C. Stevenson
A. D. Tevebaugh
Z. Tomczuk
W. D. Tuohig
D. R. Vissers
G. J. Vogel
S. Vogler
P. Walker
W. J. Walsh
A. Wantroba
D. S. Webster
I. Winsch
R. Winston
R. Yamartino
N. P. Yao
S. Zwerdling
A. B. Krisciunas
ANL Contract Copy
ANL Libraries (5)
TIS Files (6)

External:

ERDA-TIC, for distribution per UC-62 (298)
Manager, Chicago Operations Office
Chief, Chicago Patent Group
President, Argonne Universities Association
Chemical Engineering Division Review Committee:
R. C. Axtmann, Princeton U.
R. E. Balzhiser, Electric Power Research Inst.
J. T. Banchero, U. Notre Dame
D. L. Douglas, Gould Inc.
P. W. Gilles, U. Kansas
R. I. Newman, Allied-General Nuclear Services
G. M. Rosenblatt, Pennsylvania State U.
R. W. Allen, U. Maryland
B. N. Anderson, Total Environmental Action, Harrisville, NH
L. B. Anderson, Lockheed Palo Alto Res. Lab.
C. Backus, Arizona State U.
D. Baker, East Lansing, Mich.
M. D. Balcomb, Los Alamos Scientific Lab.
R. M. Banks, Lawrence Berkeley Lab.
C. S. Barnaby, Berkeley Solar Group
T. R. Beck, Electrochemical Technical Corp.
W. A. Beckman, U. Wisconsin
J. A. Belding, CONRT, USERDA
R. F. Boehm, U. Utah
P. Bos, Electric Power Research Inst.

K. W. Boer, U. Delaware
P. S. Bringham, Lawrence Berkeley Lab.
H. Buchberg, U. California, Los Angeles
E. Buzzelli, Westinghouse Electric Corp., Pittsburgh
R. Caputo, Altadena, Calif.
I. Catton, U. California, Los Angeles
B. T. Chao, U. Illinois
B. Chen, U. Nebraska
W. Christensen, Asst. for Energy Resources, The Pentagon
F. Cornford, Shuron Continental, Rochester
G. Cramer, Southern California Edison
J. E. Cummings, Electric Power Research Inst.
E. S. Davis, Jet Propulsion Lab.
F. DeWinter, Atlas Corp.
J. L. Douglas, Gould Inc.
K. Drumheller, Richland, Wash.
F. Dubin, Dubin-Mindell-Bloome, Assoc.
W. S. Duff, Colorado State U.
D. K. Edwards, U. California, Los Angeles
J. A. Eibling, Battelle Columbus Lab.
R. P. Epple, BES, USERDA
G. Ervin, Rockwell International
F. Fachat, Kaiser Aluminum & Chemical Corp.
E. A. Farber, U. Florida
R. L. French, Jet Propulsion Lab.
J. H. B. George, Arthur D. Little, Inc.
S. F. Gilman, State College, Pa.
B. Gopler, Scientific Applications, Inc.
J. C. Grosskreutz, Black and Veatch Consulting Engs.
Y. P. Gupta, E-Systems, Dallas
W. Hassenzahl, Los Alamos Scientific Lab.
H. R. Hay, Skytherm Processors Eng.
A. F. Hildenbrandt, U. Houston
J. E. Hill, National Bureau of Standards
A. S. Hirshberg, Jet Propulsion Lab.
R. M. Holdredge, Utah State U.
Dr. Jardine, Colorado Springs, Colo.
P. O. Jarvinen, Masschusetts Institute of Technology
A. Jenkins, Systems, Science and Software
P. E. Jenkins, Texas A & M U.
G. R. Johnson, Colorado State U.
H. Kausman, New York State Energy Research and Development Authority
P. A. Kittle, Rohm and Haas Co.
W. H. Klein, Smithsonian Institution
J. F. Kreider, Environmental Consulting Services, Boulder
F. Kreith, U. Colorado
Z. Lavan, Illinois Institute of Technology
Civil Engineering Laboratory, Naval Construction Battalion Center, Port Hueneme
Energy Resources Conservation and Development Commission, Sacramento
G. O. G. Lof, Colorado State U.
J. D. MacKenzie, U. California, Los Angeles
K. N. Marshall, Lockheed Research Lab.
D. K. McDaniels, U. Oregon
J. McKeown, Jr. AC, USERDA

M. Merriam, U. California, Berkeley
A. C. Meyers, Technical Environmental Resources Research Associates, Ames
C. Miller, Chamberlain Mfg. Corp., Waterloo
J. E. Minardi, U. Dayton
F. H. Morse, U. Maryland
P. W. B. Niles, Calif. Polytechnic State U.
M. C. Noland, Midwest Research Inst.
F. Notaro, Union Carbide Corp., Tonawanda
P. G. Pabil, PPG Industries, Inc., Pittsburgh
B. A. Phillips, Phillips Engineering Co., St. Joseph
J. W. Ramsey, Honeywell, Inc., Minneapolis
D. R. Reese, Wyle Laboratories, Huntsville
G. T. Reynolds, Princeton U.
R. K. Sakhuja, Thermo Electron Corp. R & D Center, Waltham
A. T. Sales, Georgia Inst. Technology
R. L. San Martin, New Mexico State U.
H. J. Schwartz, NASA Lewis Research Center
R. I. Schoen, National Science Foundation
M. K. Selcuk, Jet Propulsion Laboratory
C. Sepsy, Ohio State U.
A. M. Severson, Minneapolis, Minn.
F. F. Simon, NASA Lewis Research Center
R. H. Smith, Solergy, San Francisco
D. L. Spencer, U. Iowa
O. Stephens, General Electric Co., Bellevue, Ohio
E. Streed, National Bureau of Standards
M. Telkes, U. Delaware
E. Thomas, International Silver Co., Meriden
L. Topper, National Science Foundation
L. Vant-Hull, U. Houston
H. Volkin, Los Alamos Scientific Lab.
M. Wahlig, Lawrence Berkeley Lab.
L-C. Wen, Jet Propulsion Lab.
D. H. White, U. Arizona
R. Williams, Georgia Inst. Technology
J. W. Williamson, Vanderbilt U.
M. Wolf, U. Pennsylvania
J. I. Yellot, Arizona State U.
K. Collier, U. Maryland
A. Heller, Bell Telephone Labs.
B. L. Youtz, Olympia, Wash.
B. Shelpuk, RCA Corp., Camden
D. Ludwig, Intertech Corp.
L. T. Fan, Kansas State U.
R. Humphries, NASA Marshall Space Flight Center
D. Moeller, Sun Trac Corp., Wheeling, Ill.
P. Call, Solar Energy Research Inst.
C. Mahrok, General Services Administration
C. E. Bond, U. Illinois
G. Thodos, Northwestern U.
R. Ashby, Ministry of Mining & Natural Resources, Kingston, Jamaica
P. I. Cooper, C.S.I.R.O., Victoria, Australia
R. L. Datta, Central Salt and Marine Chemicals Research Inst., Bhavnagar, India
R. V. Dunkle, C.S.I.R.O., Victoria, Australia

J. C. Francken, U. Groningen, The Netherlands
J. T. E. Gilbert, Commission for The Environment, Wellington North, New Zealand
N. K. Gopalkrishnan, Tata Energy Research Inst., Bombay, India
M. C. Gupta, Indian Inst. Technology, Madras, India
K. G. Hollands, U. Waterloo, Canada
C. J. Hoogendorn, Technical U. Delft, The Netherlands
R. Kersten, Philips Forschungslaboratorium Aachen GmbH. Aachen, W. Germany
K. Kimura, Waseda University, Tokyo, Japan
V. Korsgaard, Technical U. Denmark, DK-2800 Lyngby
T. A. Lawland, McGill University, Canada
R. N. Morse, C.S.I.R.O., Victoria, Australia
J. Mustoe, London, England
Y. Nakajima, Kojakuin U., Tokyo
K. S. Ong, U. Malaya, Kuala Lampur
D. Proctor, P.O.B. 26, C.S.I.R.O., Victoria, Australia
W. R. Read, C.S.I.R.O., Victoria, Australia
A. Roy, U. Negev, P.O.B. 2053, Beer-Sheva, Israel
K. Saito, Osaka Inst. Technology, Osaka, Japan
B. Sesolis, U. Paris, France
H. Tabor, The Scientific Research Foundation, Jerusalem, Israel
F. Trombe, Laboratoire de l'Energie Solaire, Font Romen, France
R. Bruno, Philips Forschungslaboratorium Aachen, GmbH, Germany
W. W. S. Charters, U. Melbourne, Victoria, Australia
Salah El-Ein Hedayat, Minister of State for Research and Development, Cairo, Egypt
R. Rigopoulos, U. Patras, Greece